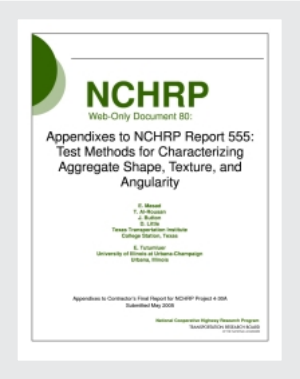

Appendixes to NCHRP Report 555: Test Methods for Characterizing Aggregate Shape, Texture, and Angularity

DETAILS

0 pages | null | PAPERBACK
ISBN 978-0-309-43656-4 | DOI 10.17226/23206

AUTHORS

NCHRP

Web-Only Document 80:

Appendixes to NCHRP Report 555: Test Methods for Characterizing Aggregate Shape, Texture, and Angularity

E. Masad
T. Al-Rousan
J. Button
D. Little
Texas Transportation Institute
College Station, Texas

E. Tutumluer
University of Illinois at Urbana-Champaign
Urbana, Illinois

Appendixes to Contractor's Final Report for NCHRP Project 4-30A
Submitted May 2005

National Cooperative Highway Research Program
TRANSPORTATION RESEARCH BOARD
OF THE NATIONAL ACADEMIES

ACKNOWLEDGMENT

This work was sponsored by the American Association of State Highway and Transportation Officials (AASHTO), in cooperation with the Federal Highway Administration, and was conducted in the National Cooperative Highway Research Program (NCHRP), which is administered by the Transportation Research Board (TRB) of the National Academies.

THE NATIONAL ACADEMIES

Advisers to the Nation on Science, Engineering, and Medicine

The **National Academy of Sciences** is a private, nonprofit, self-perpetuating society of distinguished scholars engaged in scientific and engineering research, dedicated to the furtherance of science and technology and to their use for the general welfare. On the authority of the charter granted to it by the Congress in 1863, the Academy has a mandate that requires it to advise the federal government on scientific and technical matters. Dr. Ralph J. Cicerone is president of the National Academy of Sciences.

The **National Academy of Engineering** was established in 1964, under the charter of the National Academy of Sciences, as a parallel organization of outstanding engineers. It is autonomous in its administration and in the selection of its members, sharing with the National Academy of Sciences the responsibility for advising the federal government. The National Academy of Engineering also sponsors engineering programs aimed at meeting national needs, encourages education and research, and recognizes the superior achievements of engineers. Dr. William A. Wulf is president of the National Academy of Engineering.

The **Institute of Medicine** was established in 1970 by the National Academy of Sciences to secure the services of eminent members of appropriate professions in the examination of policy matters pertaining to the health of the public. The Institute acts under the responsibility given to the National Academy of Sciences by its congressional charter to be an adviser to the federal government and, on its own initiative, to identify issues of medical care, research, and education. Dr. Harvey V. Fineberg is president of the Institute of Medicine.

The **National Research Council** was organized by the National Academy of Sciences in 1916 to associate the broad community of science and technology with the Academy's purposes of furthering knowledge and advising the federal government. Functioning in accordance with general policies determined by the Academy, the Council has become the principal operating agency of both the National Academy of Sciences and the National Academy of Engineering in providing services to the government, the public, and the scientific and engineering communities. The Council is administered jointly by both the Academies and the Institute of Medicine. Dr. Ralph J. Cicerone and Dr. William A. Wulf are chair and vice chair, respectively, of the National Research Council.

The **Transportation Research Board** is a division of the National Research Council, which serves the National Academy of Sciences and the National Academy of Engineering. The Board's mission is to promote innovation and progress in transportation through research. In an objective and interdisciplinary setting, the Board facilitates the sharing of information on transportation practice and policy by researchers and practitioners; stimulates research and offers research management services that promote technical excellence; provides expert advice on transportation policy and programs; and disseminates research results broadly and encourages their implementation. The Board's varied activities annually engage more than 5,000 engineers, scientists, and other transportation researchers and practitioners from the public and private sectors and academia, all of whom contribute their expertise in the public interest. The program is supported by state transportation departments, federal agencies including the component administrations of the U.S. Department of Transportation, and other organizations and individuals interested in the development of transportation. **www.TRB.org**

www.national-academies.org

CONTENTS

Note: The appendixes published herein are the appendixes to *NCHRP Report 555*. Readers can read or purchase *NCHRP Report 555* at http://trb.org/news/blurb_detail.asp?id=7275.

APPENDIX B
REVIEW OF AGGREGATE CHARACTERISTICS AFFECTING PAVEMENT PERFORMANCE

INTRODUCTION

Researchers have distinguished between the different aspects that constitute aggregate particle geometry or morphology and have found that it can be fully expressed in terms of three independent properties: shape (or form), angularity (or roundness), and surface texture (*1*). A schematic diagram that illustrates the differences between these properties is shown in Figure B-1. Shape, the first-order property, reflects variations in the proportions of a particle. Angularity, the second-order property, reflects variations at the corners, that is, variations superimposed on shape. Surface texture is used to describe the surface irregularity at a scale that is too small to affect the overall shape or angularity (Figure B-1). These three properties can be distinguished because of their different scales with respect to particle size, and this feature can be used to order them. Any of these properties can vary widely without necessarily affecting the other two properties.

Previous studies have used different terminology to refer to these aggregate properties (shape, angularity, and texture). In this study, the best judgment was made in relating the description of different properties discussed in the literature to the definitions of aggregate shape properties discussed above and shown in Figure B-1. Shape is used interchangeably with form throughout the study to refer to the relative proportions of a particle's dimensions. Using a unified terminology facilitates comparing the findings of different studies and analyzing the results of different test methods.

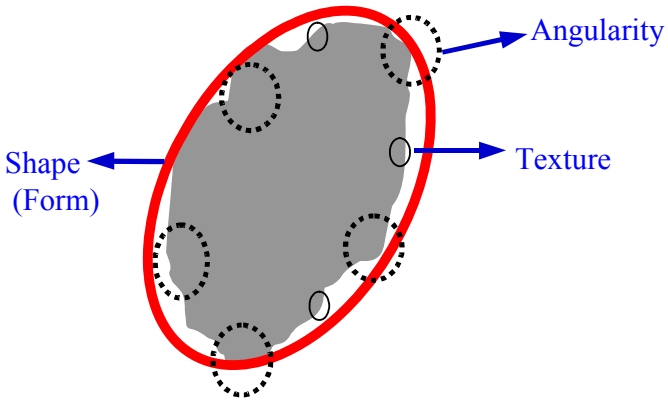

Figure B-1. Components of Aggregate Shape Properties: Shape, Angularity and Texture. (after Masad (2)).

The contents of this appendix focuses on presenting the findings of previous studies that are relevant to the influence of aggregate shape on performance of different types of pavements and on identifying aggregate characteristics affecting performance.

THE INFLUENCE OF AGGREGATE CHARACTERISTICS ON PAVEMENT PERFORMANCE

This section documents the collected and reviewed information relative to the effect of aggregate shape properties on performance of different types of pavements.

Hot-mix Asphalt Mixtures (HMA)

Many studies emphasized the role of aggregate shape in controlling the performance of asphalt mixtures, especially resistance to fatigue cracking and rutting (*3-12*). These studies conducted experiments that focused on the influence of fine aggregate, coarse aggregate, or the combined effect of fine and coarse aggregate on HMA mixture's mechanical properties and performance.

Campen and Smith (*13*) found that when crushed fine aggregates were used instead of natural rounded aggregates the stability of dense-graded HMA mixtures increased from 30 to 190 percent. They measured stability using the bearing-index test. Ishai and Gellber (*14*) used the packing volume concept developed by Tons and Goetz (*15*) to quantify the geometric irregularities of a wide range of aggregate sizes. The HMA mixtures containing different aggregates types were evaluated by Ishai and Gellber (*14*) for Marshall stability and flow, resilient modulus, and split tension strength. The results showed that there was a significant increase in stability with an increase in the geometric irregularities

of the aggregates. There was no correlation between geometric irregularities and resilient modulus or indirect tensile strength of the HMA mixtures.

Kalcheff and Tunnicliff (*16*) evaluated the effect of fine aggregate shape on HMA properties. HMA mixtures were tested using Marshall stability, repeated-load triaxial compression, static indirect tensile strength, and repeated-load indirect tensile resistance tests. They found that the use of manufactured sand instead of natural sand improved the mix behavior in terms of resistance to permanent deformation from repeated traffic loadings, tensile strength, and tensile fatigue resistance. Winford (*17*) reached the same conclusion by relating mechanical properties of HMA such as those obtained from the static confined creep test to the type of fine aggregate in the mix.

Herrin and Goetz (*18*) reported that, when the amount of crushed gravel in the coarse aggregate increased, the triaxial compressive strength of the dense-graded HMA was not significantly influenced. However, the strength of the open-graded HMA mixture increased significantly when the percentage of angular coarse aggregates was increased. Field (*19*) found a considerable increase in HMA Marshall stability due to an increase in the percentage of crushed coarse particles. The influence of crushed gravel coarse aggregate on the properties of dense-graded HMA mixtures was also investigated by Kandhal and Wenger (*20*). They found that the Marshall stability of a dense-graded mix decreased with an increase in uncrushed gravel particles. However, the differences among the mixes were not significant. They also noted that there was no significant difference in the tensile strength of HMA mixtures containing crushed and uncrushed coarse aggregates.

Sanders and Dukatz (*21*) reported on the influence of coarse aggregate angularity on permanent deformation of four interstate sections of HMA pavements in Indiana. One of

the four sections developed permanent rutting within two years of service. They found that HMA mixtures used in the binder course and the surface course of the rutted section had lower amounts of angular coarse aggregate compared to the other three sections.

Kandhal and Parker (*12*) pointed out that only a few studies have been conducted to examine the influence of flat and elongated coarse aggregate particles on HMA strength compared with studies that addressed coarse aggregate angularity. The presence of excessive flat and elongated aggregate particles is undesirable in HMA mixtures because such particles tend to break down (especially in open-graded mixtures) during production and construction, thus affecting the durability of HMA mixtures (*12*).

A study by Li and Kett (*22*) found that the dimension ratio (width to thickness or length to width) had no effect on Marshall or Hveem stability as long as the dimension ratios were less than 3:1. The permissible percentage of flat and/or elongated particles (dimension ratio exceeding 3:1), that did not adversely affect the mix stability was determined to be 30 percent or as much as 40 percent. Stephens and Sinha (*23*) reported that HMA mixes containing 30 percent or more flat particles (longest axis to shortest axis is more than or equal to three) maintained higher void contents compared to some other blends with lower percentages of flat particles. These mixes were compacted with equivalent efforts using a kneading compactor.

Some studies focused on comparing the influence of fine aggregate shape on HMA mechanical properties to the influence of coarse aggregate shape properties. Lefebure (*24*) utilized the Marshall test to measure the stability of HMA mixtures containing a crushed cubical coarse aggregate or crushed aggregates with flat and long particles combined with natural sand or crushed sand. His study concluded that fine aggregate was the most critical

component of the HMA mixture. Its quantity and characteristics controlled, to a large extent, the Marshall stability. Wedding and Gaynor (*25*) evaluated the influence of crushed coarse and fine aggregate on the Marshall stability of dense-graded HMA mixtures. Using crushed coarse aggregates caused a significant increase in stability compared with uncrushed coarse aggregates. The use of crushed fine aggregates caused an increase in stability of mixes containing uncrushed coarse aggregates. However, the use of crushed fine aggregates had a minimal effect on HMA stability when the mixes contained crushed coarse aggregates.

Foster (*26*) measured the resistance of dense-graded HMA mixtures to traffic by using test sections. He concluded that HMA mixtures containing crushed coarse aggregate showed no better performance than a mix containing uncrushed aggregates. The study attributed this finding to the crushed fine aggregate, which controlled the capacity of the mix to resist stresses induced by traffic.

The influence of shape, size, and surface texture of aggregate on stiffness and fatigue response of HMA mixture was investigated and summarized by Monismith (*4*). He indicated that aggregate characteristics affect both stiffness and fatigue response of HMA mixtures. Monismith (*4*) recommended utilizing rough-textured materials with dense gradation for thick pavements in order to increase mix stiffness and fatigue life; whereas, it might be acceptable to utilize smooth-textured aggregates in thin pavements since they produce less stiff mixtures resulting in increased fatigue life. Barksdale et al. (*7*) evaluated the effect of aggregate on rutting and fatigue of HMA mixtures. Aggregate shape was measured using image analysis techniques and the packing test developed by Ishai and Gellber (*14*). They found that aggregate shape properties obtained from the packing test

were statistically related to the rutting behavior of selected HMA mixtures. A comprehensive study by Kandhal et al. (*27*) evaluated the factors that contribute to asphalt pavement performance. They found that mixtures with less than 20 percent natural sand in the fine aggregate had better performance than mixtures with more than 20 percent natural sand. They also recommended using coarse aggregate having at least 85 percent of particles with two or more fractured faces for heavy-duty wearing and binder courses.

A study conducted at the Texas Transportation Institute related an imaging index of aggregate texture (fractal dimension) to the creep behavior of asphalt mixes (*28*). In this study, seven different aggregate blends of the same gradation but with varying amounts of crushed coarse aggregate particles were prepared. An example of the relationship between the fractal dimension and static creep compliance is shown in Figure B-2.

Figure B-3 shows the correlation between the texture of the coarse aggregates used in National Cooperative Highway Research Program (NCHRP) study 4-19 (*12*) and rutting depths of HMA measured using the Georgia Loaded Wheel Test (GLWT) (a laboratory wheel tracing device). Texture measurements were conducted using the AIMS (*29*). It can be seen that an excellent relationship exists between the texture of coarse aggregates measured using image analysis techniques and the resistance to permanent deformation.

Hydraulic Cement Concrete Mixtures

Performance of Portland cement concrete pavements (PCCP) is influenced by aggregate properties. The properties of fine and coarse aggregates used in the mix can significantly affect the pavement service life. Selection of the appropriate aggregate type

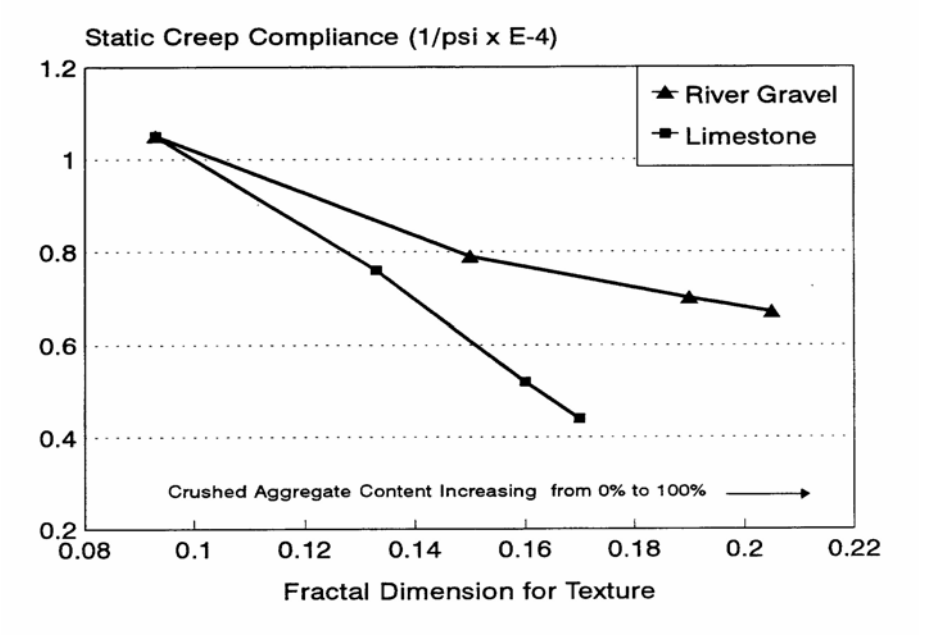

Figure B-2. Correlation between Coarse Aggregate Texture Measured Using Image Analysis and Rut Depth in the Creep Compliance of HMA (after (28)).

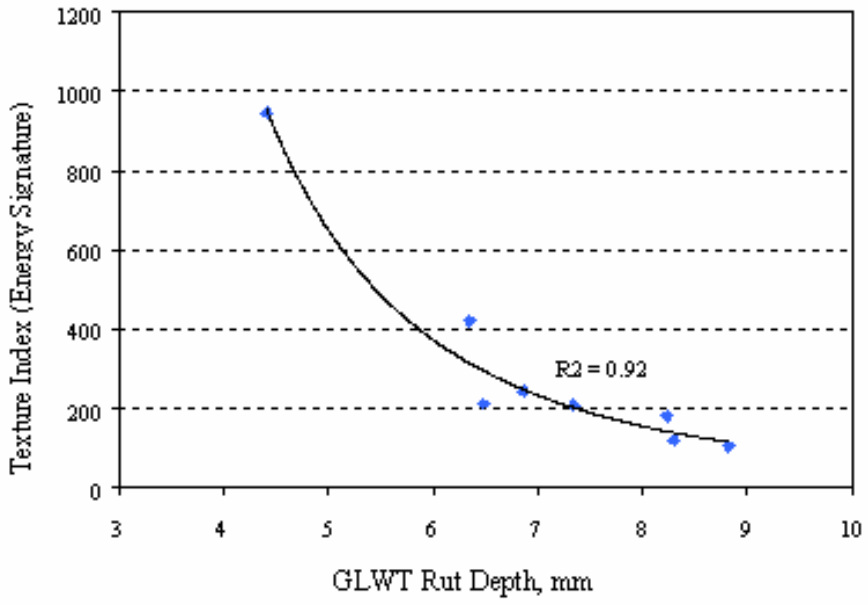

Figure B-3. Correlation between Coarse Aggregate Texture Measured Using Image Analysis and HMA Rut Depth in the Georgia Loaded Wheel Test (GWLT) (after (29)).

and properties is a key to enhancing pavement life; otherwise, poor selection can lead to premature failure in the pavement structure.

Concrete is expected to perform well during construction and service life, so PCCP will have good performance and serviceability and will last longer. The properties of the aggregate used in the concrete are expected to affect the performance parameters of both fresh and hardened Portland cement concrete (PCC). Aggregate characteristics affect the proportioning of PCC mixtures, the rheological properties of the mixtures, the aggregate-mortar bond, and the interlocking strength (load transfer) of the concrete joint/crack.

Meininger (*30*) conducted an extensive literature review and included a detailed discussion about the performance parameters of PCC used in various types of highway construction that may be affected by aggregate properties. He presented a discussion about aggregate properties related to performance parameters. Meininger (*30*) indicated that fine aggregate content and properties mostly affect the water content needed in the concrete mix. Thus, selecting or knowing the proper fine aggregate content and proper particle shape and texture will help ensure a workable, easy handling mix. Using 100 percent crushed fine aggregate reduces concrete workability significantly and makes it more difficult to place. Workable concrete is important for proper consolidation, which in turn, assures proper density, minimizes voids, and minimizes segregation at the joint areas, thus preventing spalling. An increase in the mixing water is associated with higher cement content, thus resulting in more shrinkage, which in turn, leads to more transverse cracking. As shrinkage increases, the cracks and joints open leading to reduced aggregate interlock and increased tendency toward faulting and punchouts.

Coarse aggregate particle shape and angularity are related to critical performance parameters such as transverse cracking, faulting of joints and cracks, punchouts, and spalling at joints and cracks. Using a high percentage of flat and/or elongated particles might cause problems when placing the concrete, which will result in voids and incomplete consolidation of the mix and thus contribute to spalling. If poor workability exists, then high mortar content is expected, which will lead to a high rate of drying shrinkage and transverse cracking. Although flat and elongated particles may grant good interlocking at joints or cracks, the thin particles will be easier to break, enhancing faulting in jointed concrete pavements and punchouts in continuously reinforced concrete pavements (*30*).

Coarse aggregate shape, angularity, and surface texture are believed to have a remarkable effect on the bond strength between aggregate particles and the cement paste (*31*). Weak bonding between aggregates and mortar leads to distresses in concrete pavements including longitudinal and transverse cracking, joint cracks, spalling, and punchouts (*30, 32, 33*). Kosmatka et al., (*34*) indicated that the bond strength between the cement paste and a given coarse aggregate generally increases as particles change from smooth and rounded to rough and angular. The increase in bond strength is a consideration in selecting aggregate for concrete where flexural strength is important or where high compressive strength is needed.

Kosmatka et al., (*34*) indicated that aggregate properties (shape and surface texture) affect freshly mixed concrete more than hardened concrete. Rough-textured, angular, and elongated particles require more water to produce workable concrete than do smooth and rounded aggregates. Angular particles require more cement to maintain the same water to cement ratio. However, with satisfactory gradation, both crushed and non-crushed

aggregate (of the same rock type) generally give the same strength for the same cement factor. Angular and poorly graded aggregates can be difficult to pump (*34*).

Unbound Layers

As with any other type of pavement layers, performance of unbound granular pavement base and subbase layers is greatly affected by the properties of the aggregate used. Poor performance of unbound granular base layers can result in upper pavement layer failures whether asphalt or concrete. Poor performance of an unbound granular base layer can result in different forms of distresses in an asphalt pavement, such as rutting, fatigue cracking, longitudinal cracking, depressions, corrugations, and frost heave. Poor performance of a granular base layer will result in pumping, faulting, cracking, and corner breaks in concrete pavements (*35*).

A study by Barksdale and Itani (*36*) showed significant correlation between aggregate shape properties and the resilient modulus and shear strength properties of unbound aggregates used in base layers. Saeed et al., (*35*) showed a linkage between aggregate properties and unbound layer performance. Their study showed that aggregate particle angularity and surface texture mostly affected shear strength and stiffness. Shear strength is the most important property and has a great influence on unbound pavement layer performance.

The study by Saeed et al., (*35*) revealed that lack of adequate particle angularity and surface texture is one of the contributing factors to fatigue cracking and rutting in asphalt pavements, while lack of adequate particle angularity and surface texture is a contributing factor to cracking in concrete pavement.

Rao et al., (*37*) studied the effect of aggregate shape on strength and performance of pavement layers. They indicated that the critical coarse aggregate physical properties are aspect ratio (cubical vs. flat or elongated), surface texture (smooth vs. rough surface), and angularity (sharp vs. smooth edges). While cubical coarse particles exhibit less fracturing than flat or elongated ones, angular and rough-textured coarse aggregate particles provide higher shear strength than do rounded and smooth-textured aggregate. Coarse aggregate angularity provides rutting resistance in flexible pavements as a result of improved shear strength of the unbound aggregate base and the hot mix asphalt. The interlocking of angular particles results in a strong aggregate skeleton under applied loads; whereas, round particles tend to slide by or roll past each other, resulting in an unsuitable and weaker structure.

Rao et al., (*37*) conducted a series of triaxial tests that demonstrated the influence of aggregate shape on the shear strength of several unbound materials. Figure B-4 shows the correlation between the shear strength of unbound aggregates and the angularity index (AI) measured using the University of Illinois imaging system (*37, 38*). The trend in the data presented suggests that, as the AI values increase, the angle of internal friction, ϕ, increases exponentially. The correlation between the failure deviator stress and the AI value is plotted in Figure B-4 for the three confining pressures. As the AI value of the unbound aggregate material increases, the deviator stress needed for failure also increases for each of the three confining pressures.

Based on reviewing several studies, Janoo (*39*) concluded that shape, angularity, and roughness have significant effect on base performance. He stated that several studies have shown that there can be as mush as 50 percent change in resilient modulus of base materials due to geometric irregularities of coarse and fine aggregate particles.

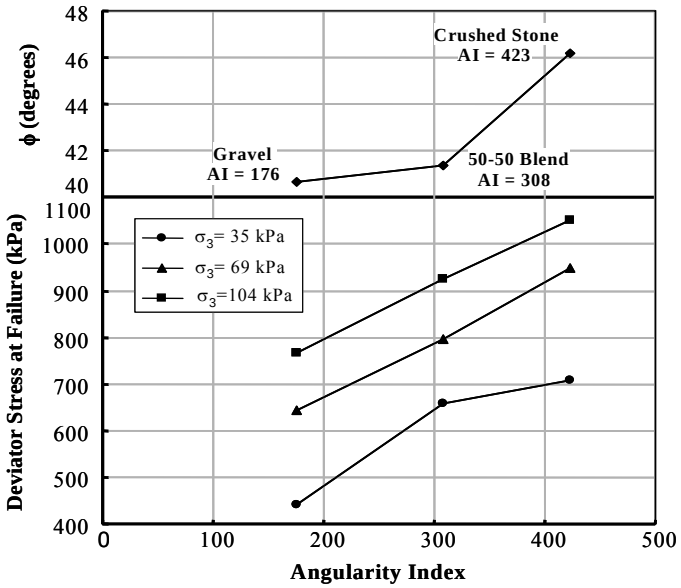

Figure B-4. Correlation between Coarse Aggregate Angularity and Shear Strength (after (37, 38).

IDENTIFYING AGGREGATE CHARACTERISTICS AFFECTING PERFORMANCE

Most of the available information on the influence of aggregate characteristics on performance emphasizes that shape, angularity, and texture play important roles in controlling performance of HMA mixtures, hydraulic cement concrete mixtures, and unbound layers. However, different shape properties influence the performance of these layers to different extents.

Most of the test methods used in the literature did not separate the influence of angularity from that of texture. Therefore, the term surface irregularity is used in this study to reflect the combined effect of angularity and texture. Previous research confirms that aggregate geometric irregularity improves the resistance of HMA to rutting. Further, aggregate surface irregularity influences the resistance of asphalt mixtures to fatigue cracking. In general, angular aggregates that increase mix stiffness are needed for thick pavements, while smooth aggregates that reduce mixture stiffness may be suitable for thin pavements to provide resistance to fatigue cracking (*4, 12*). Surface irregularity improves bonding between the aggregate surface and asphalt binder, and thus generally minimizes stripping problems.

The literature review showed that the presence of excessive flat and elongated aggregate particles is undesirable in HMA mixtures because such particles tend to break down (especially in open-graded mixtures) during production and construction, thus affecting the durability of HMA mixtures. However, only a limited number of studies were conducted to examine the influence of flat and elongated aggregate particles on performance of HMA mixture. Kandhal and Parker (*12*) recommended measuring flat,

elongated, and flat and elongated particles through measuring the three dimensions particles.

Although most available tests could not separate texture from angularity, recent studies using image analysis techniques have emphasized the significant influence that texture has on performance (*29, 40*).

The literature reviewed on the effect of aggregate properties on the performance of PCCP indicates that aggregate characteristics affect the proportioning of PCC, the rheological properties of the mixtures, the aggregate-mortar bond, and the interlocking strength of the concrete joint/crack (*30, 34*).

Aggregate particle surface irregularities have significant influence on workability and bonding between mortar and aggregates. Consequently, surface irregularities influence pavement distresses in concrete pavements including longitudinal and transverse cracking, joint cracks, spalling, and punchouts (*30, 32, 33*).

Flat and elongated particles mainly affect the workability of fresh concrete in such a way that they might cause problems when placing the concrete, which will result in voids and incomplete consolidation of the mix, and thus contribute to spalling.

Surface characteristics of aggregates used in unbound layers of pavements is a contributing factor to fatigue cracking and rutting in asphalt pavement, while lack of adequate particle angularity and surface texture is contributing factor to cracking in concrete pavement (*35, 37*).

Flat and elongated particles influence the unbound layers by increasing the anisotropic behavior of these layers. Intuitively, these flat and/or elongated particles form weak shear

planes in the direction of traffic on pavements. The stiffness anisotropy should be considered in the design of asphalt pavements (*41*).

Finally, Masad (*2*) emphasized, based on a literature review of methods used to analyze aggregate characteristics, that most analysis methods do not differentiate between angularity and texture. This creates large discrepancies in relating aggregate characteristics to performance, as aggregates that have high texture do not necessarily exhibit high angularity, especially in coarse aggregates. It is important to develop methods that are able to quantify each of the aggregate characteristics rather than a manifestation of their interaction.

REFERENCES

1. Barrett, P. J. "The Shape of Rock Particles, a Critical Review." *Sedimentology*, Vol. 27, (1980) pp. 291–303.
2. Masad, E. "Review of Imaging Techniques for Characterizing the Shape of Aggregates Used in Asphalt Mixes." Proceedings of the 9th Annual Symposium of the International Center for Aggregate Research (ICAR), Austin, TX, 2001.
3. Kalcheff, I. V. "Bituminous Concrete Properties With Large-Sized Aggregates of Different Particle Shape." *Highway Research Board Special Report 109*, Transportation Research Board, National Research Council, Washington D.C. (1968) pp. 27-32.
4. Monismith, C. L. "Influence of Shape, Size, and Surface Texture on the Stiffness and Fatigue Response of Asphalt Mixtures." *Highway Research Board 109 Special Report,* Transportation Research Board, National Research Council, Washington, D.C. (1970) pp. 4–11.
5. Benson, F. J. "Effects of Aggregate Size, Shape, and Surface Texture on the Properties of Bituminous Mixtures, a Literature Survey." *Highway Research Board 109,* Transportation Research Board, National Research Council, Washington, D.C., (1970) pp. 12–22.
6. Brown, E. R., McRea, J. L., and Crawley A. B. "Effect of Aggregates on Performance of Bituminous Concrete." *American Society for Testing and Materials ASTM STP,* Vol.1016, (1989) pp. 34-63.

7. Barksdale, R. D., Pollard C. O., Siegel, T., and Moeller, S. "Evaluation of the Effect of Aggregate On Rutting and Fatigue of Asphalt." Technical Report FHWA-AG-92-8812. Georgia Department of Transportation, Atlanta, GA, (1992).

8. Yeggoni, M., Button, J. W., and Zollinger, D. G. "Influence of Coarse Aggregate Shape and Surface Texture on Rutting of Hot-Mix Concrete." *Texas Transportation Institute Report 1244-6*, Texas A&M University, College Station, TX, (1994).

9. Chowdhury, A., Button, J. W., Kohale, V., and Jahn, D. "Evaluation of Superpave Fine Aggregate Angularity Specification." *International Center for Aggregates Research ICAR Report 201-1*, Texas Transportation Institute, Texas A&M University, College Station, TX, (2001).

10. Park, D., Chowdhury, A., and Button, J. W. "Effects of Aggregate Gradation and Angularity on VMA and Rutting Resistance." *International Center for Aggregate Research (ICAR), Report 201-3F*, Texas Transportation Institute, Texas A&M University, College Station, TX, (2001).

11. Button, J. W., Perdomo, D., and Lytton, R. L. "Influence of Aggregate on Rutting In Asphalt Concrete Pavements." *Transportation Research Record 1259*, Transportation Research Board, National Research Council, Washington D.C. (1990) pp. 141-152.

12. Kandhal, P. S., and Parker, F. Jr. "Aggregate Tests Related to Asphalt Concrete Performance in Pavements." *National Cooperative Highway Research Program Report 405*, Transportation Research Board, National Research Council, Washington, D.C. (1998).

13. Campen W. H., and Smith, J. R. "A Study of the Role Of Angular Aggregate in the Development of Stability in Bituminous Mixtures." *Association of Asphalt Paving Technologists Proceedings*, Vol. 17, (1948) pp. 114-143.

14. Ishai, I., and Gellber, H. "Effect of Geometric Irregularity of Aggregates on the Properties and Behavior of Asphalt Concrete." *Association of Asphalt Paving Technologists*, Vol. 51, (1982) pp. 494-521.

15. Tons, E., and Goetz, W. H. "Packing Volume Concepts for Aggregates." Highway *Research Record* 236, Transportation Research Board, National Research Council, Washington D.C. (1968) pp. 79-96.

16. Kalcheff, I. V., and Tunnicliff, D. G. "Effect of Crushed Stone Size and Shape on Properties Of Asphalt Concrete." *Journal of Association of Asphalt Paving Technologists*, (1982). Vol. 51, (1982) pp. 453-470.

17. Winford, J. M. "Evaluation of Fine Aggregate Particle Shape and Texture and Its Effect on Permanent Deformation of Asphalt Paving Mixtures." Ph.D. Dissertation, Dept. of Civil Engineering, Auburn University, Auburn, AL, (1991).

18. Herrin, M., and Goetz, W. H. "Effect of Aggregate Shape on Stability of Bituminous Mixes." *Highway Research Board Proceedings,* Washington D.C. (1954) pp. 293-308.

19. Field, F. "Effect of Percent Crushed Variation in Coarse Aggregates of Bituminous Mixes." *Association of Asphalt Paving Technologists Proceedings,* Vol. 27, (1958) pp. 294-322.

20. Kandhal P.S., and Wenger M.E. "Effect of Crushed Gravel Coarse Aggregate on Properties Of Bituminous Concrete." *Pennsylvania Department of Transportation. Research Report,* Harrisburg, PA, (1973) pp. 70-82.

21. Sanders, C. A., and Dukatz, E. L. "Evaluation of Percent Fracture of Hot-Mix Asphalt Gravels in Indiana." *Effect of Aggregate and Mineral Filler on Asphalt Mixture Performance,* R. C. Meininger, ed., American Society for Testing and Materials, STP 1147. Philadelphia, PA, (1992).

22. Li, M. C., and Kett, I. "Influence of Coarse Aggregate Shape on The Strength of Asphalt Concrete Mixtures." *Highway Research Record 178*, Transportation Research Board, National Research Council, Washington, D. C. (1967) pp. 93-106.

23. Stephens, J. E., and Sinha, K. C. "Effect of Aggregate Shape on Bituminous Mix Characteristics." *American Association of Paving Technologists Proceedings*, Vol. 47, (1978) pp. 434-456.

24. Lefebure, J. "Recent Investigations of Design of Asphalt Paving Mixtures." *Association of Asphalt Paving Technologists Proceedings*, Vol. 26, (1957) pp. 321-394.

25. Wedding, P. A., and Gaynor, R. D. "The Effect of Using Crushed Gravel as the Coarse and Fine Aggregate in Dense-Graded Bituminous Mixtures." *Association of Asphalt Paving Technologists Proceedings*, Vol. 30, (1961) pp. 469-492.

26. Foster, C. R. "Dominant Effect of Fine Aggregate on Strength of Dense-Graded Asphalt Mixes." *Highway Research Board Special Report 109*. Transportation Research Board, National Research Council, Washington, D.C. (1970) pp. 1-3.

27. Kandhal, P. S., Motter, J. B., and Khatri, M. A. "Evaluation of Particle Shape and Texture: Manufactured Versus Natural Sands." *Transportation Research Record 1301*, Transportation Research Board, National Research Council, Washington D.C. (1991) pp. 48-67.

28. Yeggoni, M., Button, J.W., and Zollinger, D.G. "Fractals of Aggregates Correlated with Creep in Asphalt Concrete." *Journal of Transportation Engineering (ASCE)*, Vol. 122, No. 1, (1996) pp. 22-28.

29. Fletcher, T., Chandan, C., Masad, E., and Sivakumar, K. "Measurement of Aggregate Texture and Its Influence on HMA Permanent Deformation." *Journal of Testing and Evaluation, American Society for Testing and Materials, ASTM*, Vo. 30, No. 6, (2002) pp. 524-531.

30. Meininger, R. C. "Aggregate Test Related to Performance of Portland Cement Concrete Pavement." *National Cooperative Highway Research Program Project 4-20A Final Report.* Transportation Research Board, National Research Council, Washington, D.C (1998).

31. Mindness, S., and Young, J. F., *Concrete*. Prentice Hall Inc., Englewood Cliffs, NJ (1981).

32. Fowler, D. W., Zollinger, D. G., Carrasquillo, R. L., and Constantino, C. A. *Aggregate Tests Related to Performance of Portland Cement Concrete*, Phase 1 Unpublished Interim Report, National Cooperative Highway Research Program (NCHRP) Project 4-20, Lincoln, NE (1996).

33. Folliard, K. J. "Aggregate Tests Related to Performance of Portland Cement Concrete Pavements." *National Cooperative Highway Research Program Project 4-20B*, Phase 1 Interim Report, Austin, TX (1999).

34. Kosmatka, S. H., Kerkhoff, B., and Panarese, W. C. *Design and control of concrete mixtures*, 14th edition, Portland Cement Association, Skokie, IL (2002).

35. Saeed, A., Hall, J., and Barker, W. "Performance-Related Tests of Aggregates for Use in Unbound Pavement Layers." *National Cooperative Highway Research Program Report 453*, Transportation Research Board, National Research Council, Washington, D.C (2001).

36. Barksdale, R. D., and Itani, S. Y. "Influence of Aggregate Shape on Base Behavior." *Transportation Research Record 1227*, Transportation Research Board, National Research Council, Washington, D.C. (1994) pp. 171-182.

37. Rao, C., Tutumluer, E., and Kim, I. T. "Quantification of Coarse Aggregate Angularity Based on Image Analysis." *Transportation Research Record 1787*, Transportation Research Board, National Research Council, Washington, D.C. (2002) pp. 117-124.

38. Rao, C. "Development of 3-D Image Analysis Techniques to Determine Shape and Size Properties of Coarse Aggregate." Ph.D. Dissertation, Dept. of Civil Engineering, University of Illinois at Urbana-Champaign, Urbana, IL (2001).

39. Janoo, V. C. "Quantification of Shape, Angularity, and Surface Texture of Base course Materials." *U.S. Army Corps of Engineers Special Report 98-1*, Cold Regions Research & Engineering Laboratory, Hanover, NH (1998).

40. Masad, E. "The Development of a Computer Controlled Image Analysis System for Measuring Aggregate Shape Properties." *National Cooperative Highway Research Program NCHRP-IDEA Project 77 Final Report*, Transportation Research Board, National Research Council, Washington, D.C (2003).

41. Tutumluer, E., and Thompson, M. R. "Granular Base Moduli for Mechanistic Pavement Design." *ASCE Airfield Pavement Conference Proceedings*, Seattle, WA (1997) pp. 33-47.

APPENDIX C
IMAGE ANALYSIS METHODS FOR CHARACTERIZING AGGREGATE SHAPE PROPERTIES

IMAGE ANALYSIS METHODS FOR CHARACTERIZING AGGREGATE SHAPE PROPERTIES

Several investigations have been conducted on the use of imaging technology to quantify aggregate shape properties and relate them to the performance of pavement layers. Some of these studies focused on developing procedures to describe shape (*1*, *2*, *3*, *4*, *5*, *6*, *7*, *8*), angularity (*9*, *10*, *11*, *12*, *13*, *14*, *15*), and surface texture (*14, 16*, *17*, *18*, *19*, *20*, *21*).

This section describes, in general terms, most of the image analysis methods used to characterize particle shape, angularity, or texture. The discussion provided in this section on the analysis methods is largely taken from Masad (14), Fletcher (22) , and Chandan et al. (21).

Typical Analysis of Shape

Sphericity

In order to properly characterize the shape of an aggregate particle, information about three dimensions of the particle is necessary {longest dimension, [d_l], intermediate dimension, [d_i], and shortest dimension, [d_s]). A number of indices have been proposed for measuring shape that relate the ratio of two dimensions, such as elongation and flatness. Sphericity and shape factor are indices that are expressed in terms of three dimensions (*23*).

$$\text{Sphericity} = \sqrt[3]{\frac{d_s * d_i}{d_l^2}} \quad \text{(C-1)}$$

$$\text{Shape Factor} = \frac{d_s}{\sqrt{d_l * d_i}} \quad \text{(C-2)}$$

Form Factor

Form factor is widely used measure of shape in two-dimensions (2-D) and is expressed by the following equation:

$$\text{Form Factor} = \frac{4\pi A}{P^2} \tag{C-3}$$

where P and A are the perimeter and area of a particle, respectively. Form factor is equal to unity for a circular-shaped particle.

Roundness

The inverse of the form factor, Equation (C-3), which is known as roundness (ROUND) can also be used. Some analysis systems use other tems to describe form factor. The Camsizer system, for example, uses the term sphericity (SPHT) to describe this same term (roundness). As in shape factor, a circular object will have a roundness value of 1.0, and other shapes will have roundness values greater than 1.0.

Form Index

Form index was proposed by Masad et al., (*24*) to describe shape (or form) in 2-D. It uses incremental changes in the particle radius. The length of a line that connects the center of the particle to the boundary of the particle is termed radius. Form index is expressed by the following equation:

$$\text{Form Index} = \sum_{\theta=0}^{\theta=360-\Delta\theta} \frac{\left|R_{\theta+\Delta\theta} - R_{\theta}\right|}{R_{\theta}} \tag{C-4}$$

where θ is the directional angle and R is the radius in different directions. By examining Equation (C-4), it will be noted that, if a particle was a perfect circle, the form index would be

zero. Although the form index is based on 2-D measurements, it can easily be extended to analyze the 3-D images of aggregates.

Form Index (Fourier Series)

Fourier series can be used to analyze the shape, angularity, and texture of aggregates. Each aggregate profile, defined by the function *R(θ)*, can be analyzed using Fourier series coefficients as follows:

$$R(\theta) = a_{\circ} + \sum_{n=1}^{\infty}\left[a_n \cos(n\theta) + b_n \sin(n\theta)\right] \tag{C-5}$$

where a_n and b_n are the Fourier coefficients. The function *R(θ)* traces out the distance to the boundary from a central point as a function of the angle θ, $0^o < \theta < 360^o$. Obviously, *R(θ)* is a periodic function. These coefficients can be evaluated using the following integrals:

$$a_{\circ} = \frac{1}{2\pi}\int_0^{2\pi} \mathrm{R}(\theta)\,\mathrm{d}\theta \tag{C-6}$$

$$a_n = \frac{1}{\pi}\int_0^{2\pi} R(\theta)\cos(n\theta)\,d\theta \qquad n = 1, 2, 3, \ldots. \tag{C-7}$$

$$b_n = \frac{1}{\pi}\int_0^{2\pi} R(\theta)\sin(n\theta)\,d\theta \qquad n = 1, 2, 3, \ldots. \tag{C-8}$$

If *R(θ)* is only known numerically at a discrete number of angles, the above integrals can be written using summations as follows:

$$a_{\circ} = \frac{1}{2\pi}\sum_{\theta=0}^{2\pi-\Delta\theta}\left(\frac{R(\theta+\Delta\theta)+R(\theta)}{2}\right) \tag{C-9}$$

$$a_n = \frac{1}{\pi}\sum_{\theta=0}^{2\pi-\Delta\theta}\left(\frac{R(\theta+\Delta\theta)+R(\theta)}{2}\right)\left(\sin n(\theta+\Delta\theta) - \sin n\theta\right) \tag{C-10}$$

$$b_n = \frac{1}{\pi}\sum_{\theta=0}^{2\pi-\Delta\theta}\left(\frac{R(\theta+\Delta\theta)+R(\theta)}{2}\right)\left(-\cos(\theta+\Delta\theta)+\cos n\theta\right) \quad \text{(C-11)}$$

where $R(\theta)$ is measured only at predefined increments, and θ takes on values from 0 to $(2\pi - \Delta\theta)$ with an increment $\Delta\theta$ of about 4^o. The higher the value of n used in Equation (C-5), the better the actual particle profile is reproduced. Wang et al., (*25*) formulated shape signatures using the a_n and b_n coefficients as follows:

Form Signature: $n \leq 4$

$$\alpha_s = \sum_{j=1}^{4}\left[\left(\frac{a_n}{a_0}\right)^2+\left(\frac{b_n}{a_0}\right)^2\right] \quad \text{(C-12)}$$

The characteristics (shape, angularity, and texture) can all be represented by the same function and at the same time can be differentiated by the frequency magnitudes of the harmonics used to capture a particle boundary. Shape (or form) is captured using harmonics with lower frequency than texture and angularity.

Flat and Elongated Ratio

Another way of presenting the shape of a particle is by using flat and elongated ratio (FER). FER represents the ratio between the longest dimension and the shortest dimension of a particle which is perpindicular to the longets dimension.

Aspect Ratio

Aspect ratio (ASPCT), which is similar to FER ratio but usually used for 2-D projections, is used to describe the shape of particles. It is the ratio of the major axis to minor axis of the ellipse equivalent to the object, which is a particle image in this case. The equivalent ellipse is

supposed to have the same area as the particle image and first and second degree moment. Aspect ratio is always equal to or greater than 1.0, since it is defined as (major axis/minor axis).

Breadth to Width Ratio

Breadth to width ratio can be used to describe the shape of aggregate particles. The Camziser system uses the following equation to calculate this ratio:

$$\text{Ratio of Breadth to Width} = b/l = \frac{\min(x_c)}{\max(x_{Fe})} \quad \text{(C-13)}$$

Where, x_c is the maximum chord, and x_{Fe} is the Feret diameter, both determined from up to 32 directions for each particle. Feret diameter is the distance between two tangents placed 90^o to the measuring direction and touching the particle.

Symmetry

Symmetry is another term that some imaging systems use to describe aggregate shape. Symmetry of an aggregate particle can be given by:

$$\text{Symmetry} = \frac{1}{2}\left[1 + \min\left(\frac{r_1}{r_2}\right)\right] \quad \text{(C-14)}$$

where r_1 and r_2 are the distances of the center of gravity to the edge in a given direction, i.e., maximum diameter = $r_1 + r_2$.

Typical Analysis of Angularity

Analysis methods for angularity have used mainly black and white images of 2-D projections of aggregates. The assumption here is that the angularity elements in 2-D are a good measure of the 3-D angularity. It should be noted that the image resolution required for

angularity analysis can easily be achieved using automated systems for capturing images. Masad et al., (*24*) specified that an image resolution with a pixel size less than or equal to 1% of the particle diameter is required for angularity analysis.

Fourier Series Analysis of Angularity

As mentioned earlier in the previous section, Fourier series analysis can be used to analyze angularity of aggregates. The shape signature for angularity as formulated by Wang et al. (*25*) is given by:

Angularity Signature: $5 \leq n \leq 25$

$$\alpha_r = \sum_{j=5}^{25} \left[\left(\frac{a_n}{a_0} \right)^2 + \left(\frac{b_n}{a_0} \right)^2 \right] \qquad \text{(C-15)}$$

where a_0, a_n, and b_n are found using Equations (C-9 through C-11). Angularity is captured using harmonics with frequencies that are higher than form and lower than texture.

Surface Erosion-Dilation Technique

The erosion-dilation technique has been used to capture fine aggregate angularity and even surface texture (*18*). Erosion-dilation is well known in image processing, where it is used both as a smoothing technique (*26*) and a shape classifier (*27*). Erosion is a morphological operation in which pixels are removed from the image according to the number of pixels surrounding it with different color (*24*). Erosion can be visualized as a fire burning inward from the periphery of an object, in order to shrink the object to a skeleton or a point (*28*). Layer-by-layer erosion tends to smooth a particle surface.

Dilation is the opposite of the erosion. A layer of pixels is added around the periphery of the eroded image to form a simplified version of the original object. An image does not necessarily need to be restored to its original state after a number of erosion and dilation cycles (*29*). Surface angularities may be lost under erosion and will not be restored during dilation since there is no seed pixel from which the dilation can build (*30*). Following this logic, one can state that the area of the object lost after erosion and dilation is "proportional" to the angularity of the particle, assuming that no particles are lost during the procedure. Aggregate particle angularity is measured by the area lost during the erosion-dilation process and is expressed as a percentage of the total area of the original particle, which is described by the following expression:

$$\text{Surface Parameter} = \frac{A_1 - A_2}{A_1} * 100\% \qquad \text{(C-16)}$$

where A_1 and A_2 are the area of the object before and after applying the erosion-dilation operations, respectively (Figure C-1). A particle with more angularity would lose more area than that of a smooth one; therefore, the surface parameter would be higher. Masad and Button (*18*) found that this parameter correlated to angularity of a particle at low resolutions and to surface texture of a particle at higher resolutions.

Fractal Behavior Technique

In its simplest form, fractal behavior is defined as the self-similarity exhibited by an irregular boundary when captured at different magnifications. Fractal behavior has many applications in science (*31*), particularly for describing the shape of natural objects (e.g., clouds, body organs, rocks, etc.). Smooth boundaries erode (or dilate) at a constant rate. However, irregular or fractal boundaries have more pixels touching opposite-color neighbors, and, hence, they do not erode (or dilate) uniformly. This effect has been used to estimate fractal dimensions,

and, consequently, angularity along the object boundary. The basic idea for measuring a fractal dimension by image analysis came from the Minkowski definition of a fractal boundary dimension (*32*). This procedure was used by Masad et al., (*12*) to characterize the angularity of a wide range of aggregates used in asphalt mixes. The procedure is depicted in Figure C-1.

The first step is to apply a number of erosion and dilation operations on the original image as shown in Figure C-1(a), (b), and (d). Then, the eroded and dilated images are combined using the logical operator (Ex-OR). Using this operator, the two images (b and d) are compared and pixels that have black color representing aggregate and are at the same location on both images are removed, as shown in Figure C-1(e). By doing so, the pixels retained on the final image (Figure C-1(e)) are only those removed during erosion and added during dilation. These pixels form a boundary, which has a width proportional to the number of erosion-dilation cycles and surface angularity (Figure C-1 (e)).

The procedure continues by varying the number of erosion-dilation cycles and measuring the increase in the effective width of the boundary (total number of pixels divided by boundary length and number of cycles). Then, the effective width is plotted versus the number of erosion-dilation cycles on a log-log scale. For a smooth boundary, the effective width to number-of-cycles relationship shows no trend; that is, the effective width remains constant at different numbers of cycles. However, for a boundary with angularity, the graph would show a linear variation, where the slope gives the fractal length of the boundary.

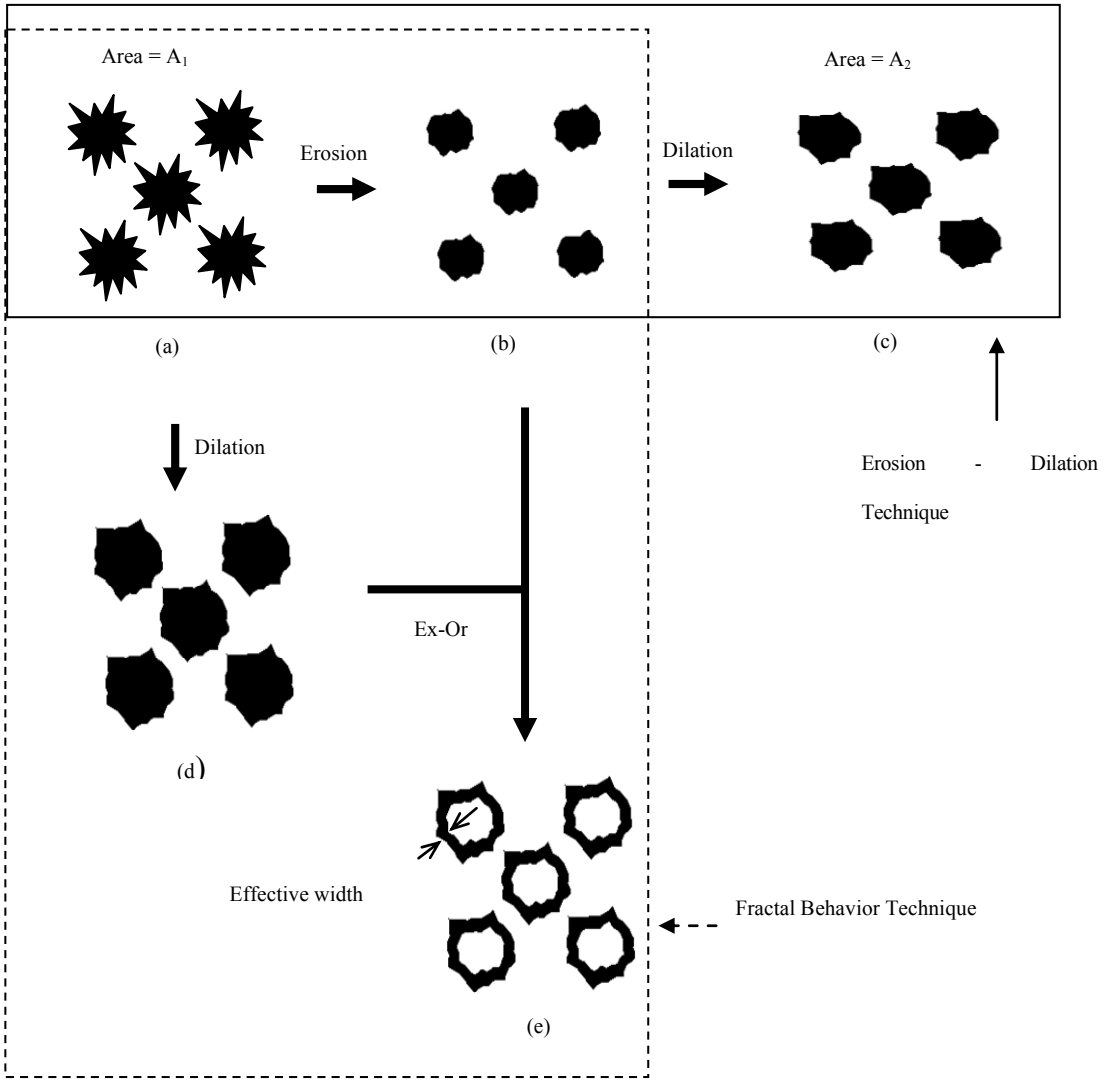

Figure C-1. Illustration of the Erosion-Dilation and Fractal Behavior Method (after (24)).

Hough Transform

Hough Transform is another technique used to recognize co-linearity in pixels that form the particle outline (*33*). This technique has been successfully implemented in the medical field and in the analysis of aerial images. By detecting and measuring the length of any straight lines in a 2-D image and the angle between them, angularity of a particle can easily be determined.

Wilson et al., (*34*) used the Hough Transform to develop an index for quantifying aggregate angularity. This transform was used to determine the longest line on the outline of particle images at each possible direction $A(\theta)$. Then, the length of the longest line, A_{Max}, in all directions and the average length of the line, A, which also corresponds to the longest line on the edge of the particle are computed. Angularity is then quantified by the index:

$$\text{Hough Transform Shape Index} = 1 - \frac{A}{A_{Max}} \qquad \text{(C-17)}$$

Wilson and Klotz (*10*) noted that, if only one or two lines dominated the particle, the value approached 1.0. However, if the particle was rounded or irregular, then all of the straight lines are short and close to the average and the index approached 0.0. Therefore, the index approaches 0.0 for rounded particles and is typically greater than 0.6 for angular particles.

Gradient Method

The main idea behind this method is that, at sharp corners of the surface of a particle image, the direction of the gradient vector for adjacent points on the surface changes rapidly. On the other hand, the direction of the gradient vector for rounded particles changes slowly for adjacent points on the surface.

The gradient-based method for measuring angularity consists of the following steps. The acquired image is first thresholded to get a binary image. This is followed by the boundary-

detection step. Next, the gradient vectors at each surface point are calculated, using a Sobel mask that operates at each point on the surface and its eight nearest neighbors (*21*).

The Sobel operator performs a 2-D spatial gradient measurement on an image and emphasizes regions of high spatial gradient that are located at the surface. The Sobel operator picks up the horizontal (G_x) and vertical (G_y) running edges in an image. These can then be combined to find the absolute magnitude of the gradient at each point and the orientation of the gradient. The angle of orientation of the edge (relative to the pixel grid) that results in the spatial gradient is given by:

$$\theta(x, y) = \tan^{-1}\left(\frac{G_x}{G_y}\right) \tag{C-18}$$

For the angularity analysis, the angle of orientation values of the edge points (θ) and the magnitude of the difference in these values ($\Delta\theta$) for adjacent points on the edge are calculated to describe how sharp or how rounded the corner is. Figure C-2 illustrates the method of assigning angularity values to a corner point on the edge. The angularity values for all the boundary points are calculated, and their sum is accumulated around the edge to finally form a measure of angularity, which is denoted the gradient index (GI) (*21*):

$$GI = \sum_{i=1}^{N-3} \left|\theta_i - \theta_{i+3}\right| \tag{C-19}$$

where i denotes the i^{th} point on the edge of the particle, and N is the total number of points on the edge of the particle.

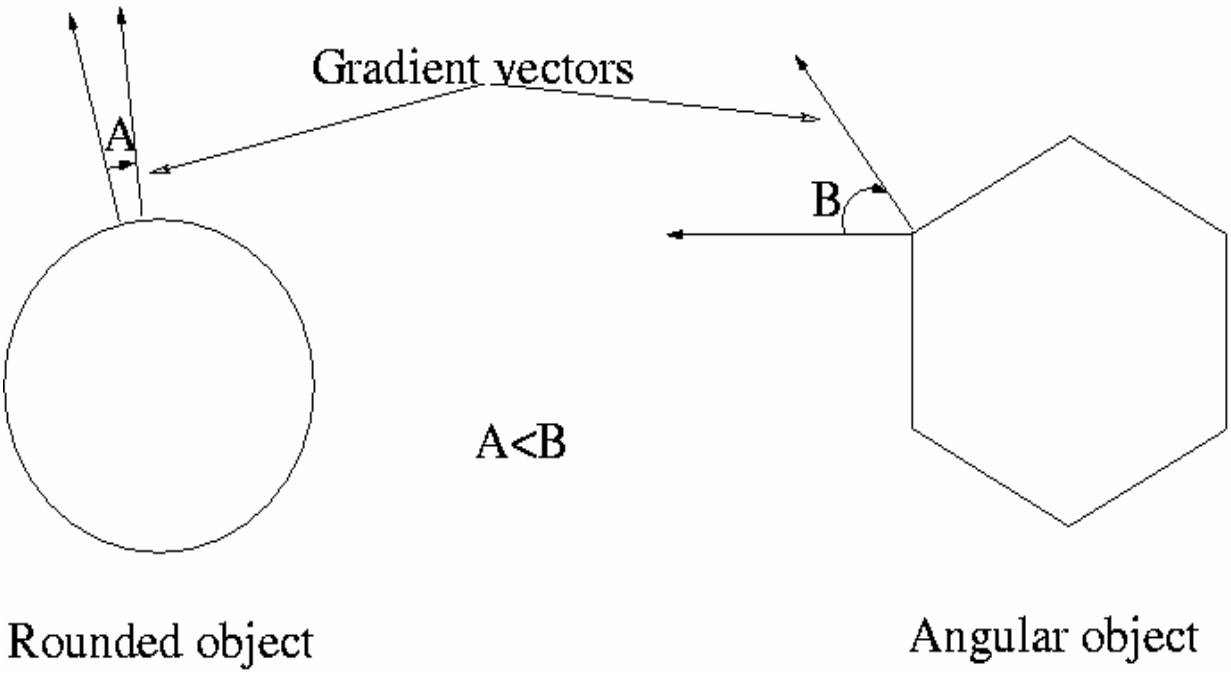

Figure C-2. Illustration of the Difference in Gradient between Particles (after (21)).

Direct Measurements of Particle Dimensions

Kuo and Freeman (*13*) (2000) proposed an angularity parameter, which is expressed by the following equation:

$$\text{Angularity Parameter} = \left(\frac{P_{convex}}{P_{ellipse}} \right)^2 \quad \text{(C-20)}$$

where $P_{ellipse}$ is the perimeter of an equivalent ellipse (i.e., an ellipse with the same longest and shortest axes of a particle), and P_{convex} is the perimeter of the bounding polygon.

Angularity Index

Masad et al,. (*24*) proposed the angularity index, which is described by the following equation:

$$\text{Angularity Index} = \sum_{\theta=0}^{\theta=360-\Delta\theta} \frac{\left| R_{P\theta} - R_{EE\theta} \right|}{R_{EE\theta}} \quad \text{(C-21)}$$

where $R_{P\theta}$ is the radius of the particle at a directional angle, θ. $R_{EE\theta}$ is the radius of an equivalent ellipse at the same θ. The index relies on the difference between the radius of a particle in a certain direction and a radius of an equivalent ellipse taken in the same direction as a measure of angularity. By normalizing the measurements to the ellipse dimensions, the effect of form on angularity is minimized (*24*).

Outline Slope Method

Based on image analysis from the images captured by the University of Illinois Aggregate Imaging Analyzer (UIAIA), a quantitative angularity index (AIUI) was developed (*15*). The AIUI methodology is based on tracing the change in slope of the particle image

outline obtained from each of the top, side, and front images. Accordingly, the AIUI procedure first determines an angularity index value for each 2-D image. Then, a final AIUI is established for the particle by taking a weighted average of its angularity determined for all three views.

To determine angularity for each 2-D projection, an image outline based on aggregate camera view projection and its coordinates are first extracted. Next, the outline is approximated by an *n*-sided polygon, as shown in Figure C-3. The angle subtended at each vertex of the polygon is then computed. Relative change in slope of the n sides of the polygon is subsequently estimated by computing the change in angle (β) at each vertex with respect to the angle in the preceding vertex. The frequency distribution of the changes in the vertex angles is established in 10^o class intervals. The number of occurrences in a certain interval and the magnitude are then related to the angularity of the particle profile.

Equation (C-22) is used for calculating angularity of each projected image. In this equation, *e* is the starting angle value for each 10^o class interval, and *P(e)* is the probability that change in angle α has a value in the range *e* to (*e+10*).

$$Angularity = A = \sum_{e=0}^{170} e * P(e) \tag{C-22}$$

The UIAI of a particle is then determined by averaging the angularity values (see Equation C-23) calculated from all three views when weighted by their areas as given in the following equation:

$$UIAI = \frac{A(front) * Area(front) + A(top) * Area(top) + A(side) * Area(side)}{Area(front) + Area(top) + Area(side)} \tag{C-23}$$

The final UIAI value for the entire sample is simply an average of the angularity index values of all the particles weighted by the particle weight, which measures overall degree changes on the boundary of a particle.

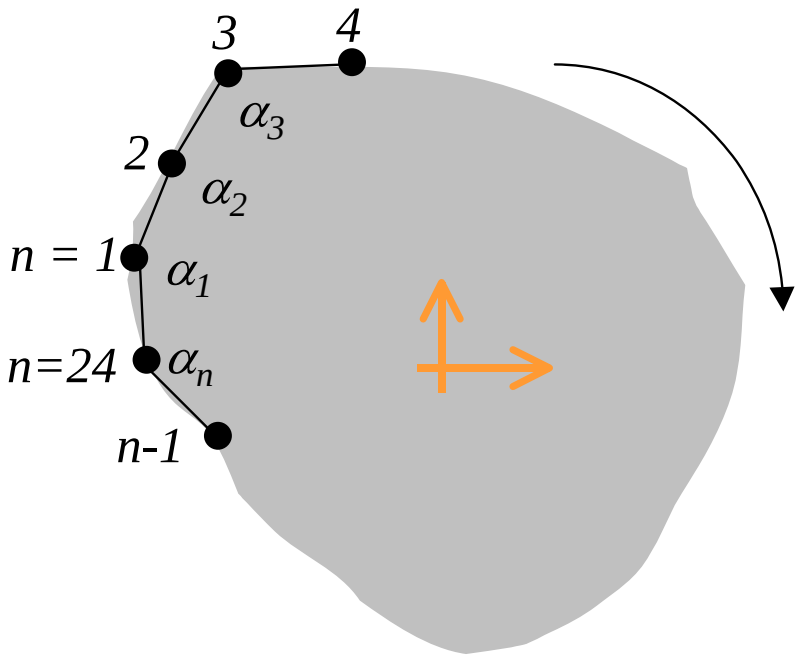

Figure C-3. Illustration of an n-Sided Polygon Approximating the Outline of a Particle (after (15)).

Convexity

Convexity is another parameter that can used to describe angularity of aggregate particles. Convexity can be calculated using the following formula:

$$\text{Convexity} = Conv = \sqrt{\frac{A_{Particle}}{A_{Convex}}} \quad \text{(C-24)}$$

Where $A_{Particle}$ is the area of the real projection of the particle, and A_{Convex} is the area of the convex particle's projection.

Minimum Average Curve Radius

This method is described by Maerz (*35*) and illustrated in Figure C-4. In this method, aggregate angularity is defined as the minimum average curve radius of the individual particles. Maerz (*35*) described the following procedure to calculate the minimum average curve radius: The radius of a circle containing three points on the profile is calculated from the array of x, y points, each point separated by 10 pixels. An instantaneous curve radius is determined for each point on the profile in this manner, creating an array of curve radii. Then the array of curve radii values are smoothed by a moving average filter. A 5-point Gaussian low-pass filter is used (see Figure C-5). The array of smoothed curve radii is examined to find local minimal in the curve radius function. A test is performed to ensure that a corner of the aggregate piece does not result in more than one local minimum. Then the list of local minimum curve radii is ordered from smallest to largest. The averages of the four smallest curve radii are averaged to produce the minimum average curve radius of the individual piece.

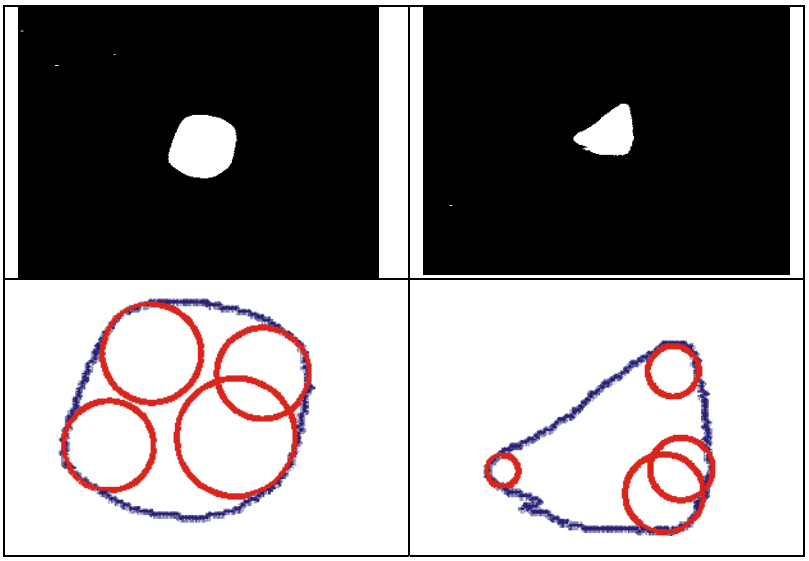

Figure C-4. Average Minimum Curve Radius Calculations. Left: Rounded Aggregate. Right: Angular Aggregate. Bottom: Aggregate Profile with Inscribed Curve Radii (after (35)).

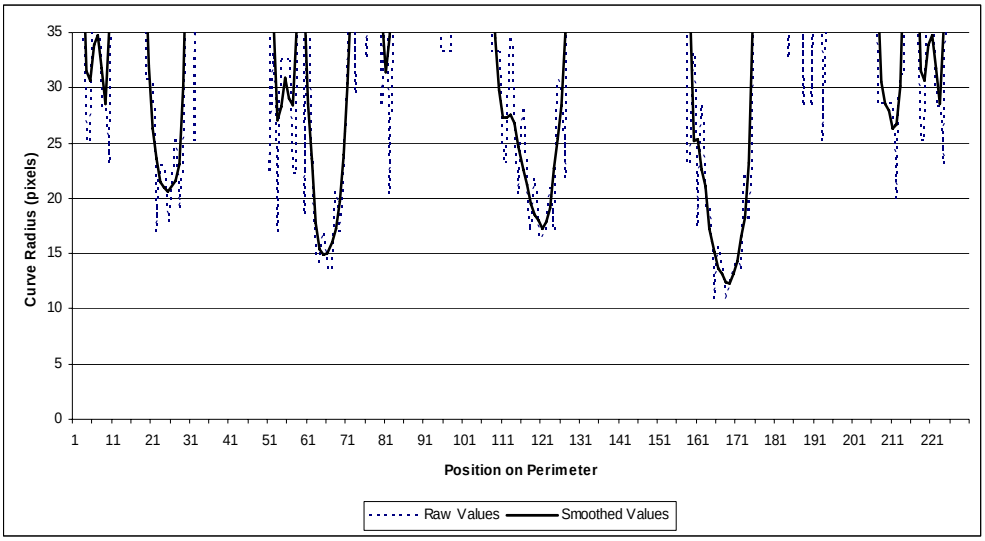

Figure C-5. Curve Radius Measurements around the Profile of the Rounded Particle in Figure C-4; Raw and Smoothed Values (after (35)).

Typical Analysis of Texture

The analysis of texture has been performed using both black and white images and gray images. The main disadvantage of using black and white images is the high resolution required for capturing images, which makes it difficult to use automated systems. In addition, the majority of texture details are lost when a gray image is converted to black and white. The analysis of gray images has the advantage of analyzing more texture data at the surface of a particle, leading to detailed information about texture. However, the main challenge facing this technique is the influence of natural variation of color on gray intensities and, consequently, texture analysis. Some image analysis techniques have the potential to separate the actual texture from color variations. This section discusses some of the techniques used to analyze the texture of aggregates.

Fourier Series Analysis of Texture

As mentioned in the previous section, Fourier series analysis can be used to analyze texture of aggregates. The shape signature for texture, as formulated by Wang et al. (*25*), is given by:

Texture Signature: $26 \leq n \leq 180$

$$\alpha_t = \sum_{j=26}^{180} \left[\left(\frac{a_n}{a_0} \right)^2 + \left(\frac{b_n}{a_0} \right)^2 \right] \qquad \text{(C-25)}$$

where a_0, a_n, and b_n are found using Equations C-9 to C-11. Texture is captured using harmonics with frequencies that are higher than angularity and shape.

Intensity Histogram Method

An intensity histogram evaluates the variation in the gray intensity of the gray-scale image over the entire image. The mean and standard deviation of the variations are the output from the intensity histogram. There is a correlation between the standard deviation of gray intensity and the surface texture of the particle (*24*). Standard deviations are typically much lower for smooth particles than for rough particles. Figure B-6 shows images of smooth and rough particles and their intensity histograms.

Fast Fourier Transform Method

This is a well-known method in the sciences for converting data from the time or spatial domain to the frequency domain. Dominant frequencies become apparent when a Fast Fourier Transform (FFT) is applied to a gray-scale image. Frequency is a measure of reoccurrence of a distinct gray level intensity in the image. The resulting FFT image consists of points of different gray levels, where the distance of a point from the center represents the frequency and the gray level in the FFT image corresponds to the peak intensity at a given frequency (*32*). The number of dominant peaks in the FFT has been found to be a measure of the surface texture (*24*) (Figure C-6).

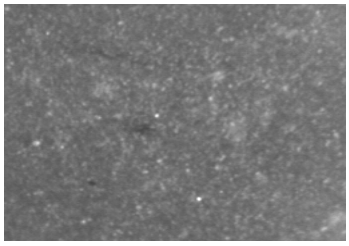

(a) Smooth texture

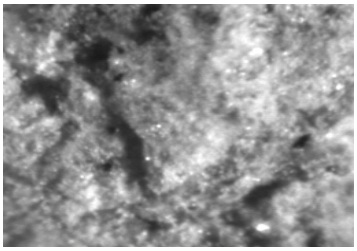

(b) Rough texture

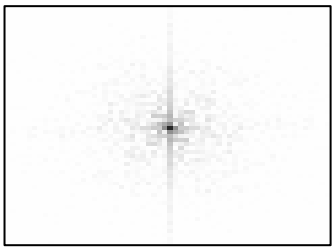

(c) FFT of smooth texture

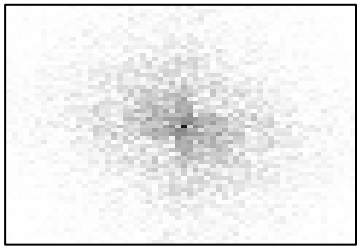

(d) FFT of rough texture

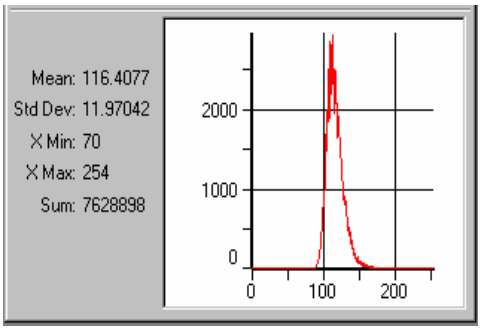

(e) Histogram of smooth texture

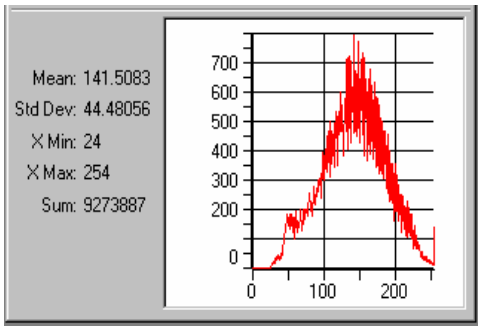

(f) Histogram of rough texture

Figure C-6. Images of Smooth-and Rough-Textured Aggregates and their Fast Fourier Transforms and Histograms (after (24)).

Wavelet Analysis

Texture in an image is represented by the local variation in the pixel gray intensity values. Although there is no single scale that represents texture, the histogram and FFT analyses of texture capture only a single scale. Wavelet theory offers a mathematical framework for multi-scale image analysis of texture (*36*). This is advantageous to determine the texture scale or a combination of them that has the most influence on the aggregate performance in pavement layers

The wavelet transform works by mapping an image onto a low-resolution image and a series of detail images. An illustration of the method is presented here with the aid of Figure B-7. The original image is shown in Figure C-7(a). It is decomposed into a low-resolution image (Image 1 in Figure C-7(b)) by iteratively blurring the original image. The remaining images contain information on the fine intensity variation (high frequency) that was lost in Image 1. Image 2 contains the information lost in the y-direction, Image 3 has the information lost in the x-direction, and Image 4 contains the information lost in both x- and y-directions. Image 1 in Figure C-7(b) can be further decomposed similar to the first iteration, which gives a multi-resolution decomposition and facilitates quantification of texture at different scales. An image can be represented in the wavelet domain by these blurred and detailed images. The texture parameter used is the average energy on Images 2, 3, and 4 at each level. Texture index is taken at a given level as the arithmetic mean of the squared values of the detail coefficients at that level *(*level 6 is used*)*:

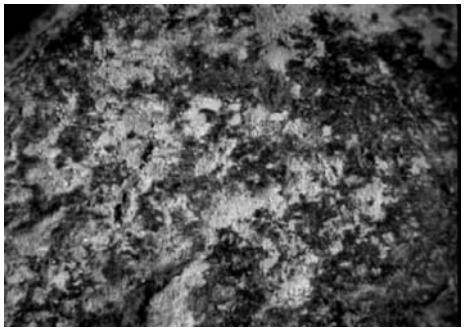

(a)

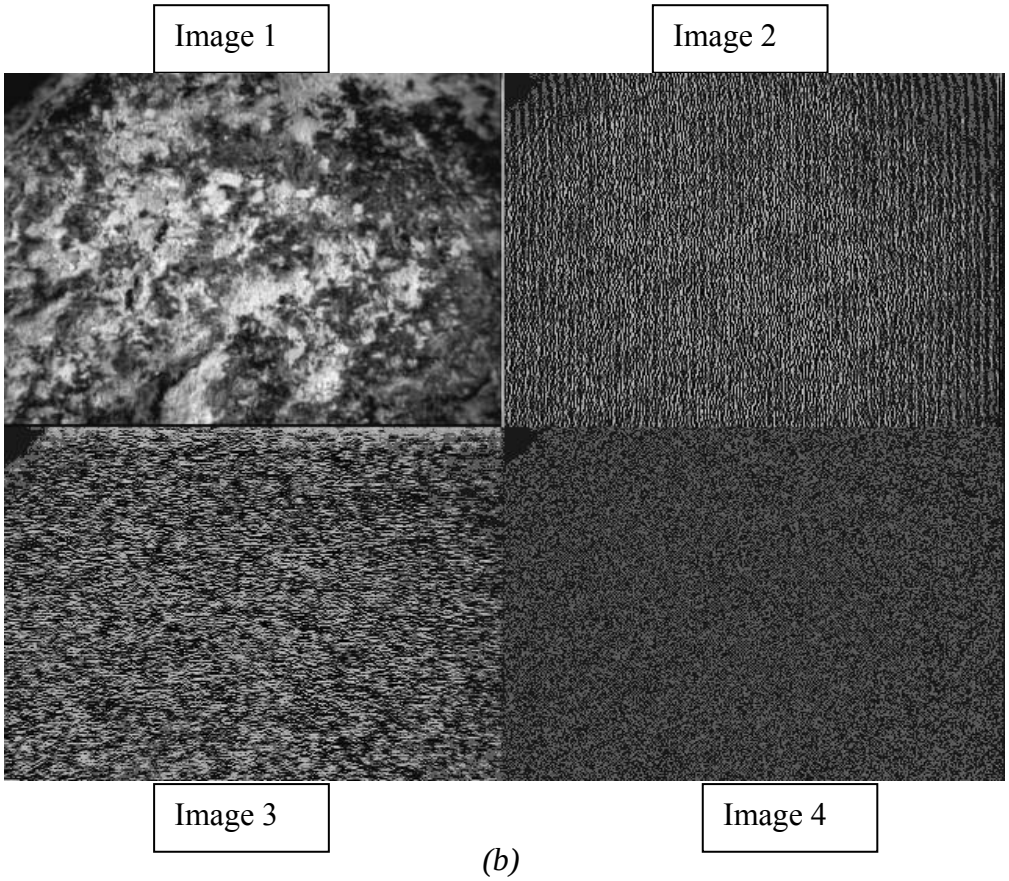

(b)

Figure C-7. Illustration of the Wavelet Decomposition (after (21)).

$$Texture\ Index_n = \frac{1}{3N}\sum_{i=1}^{3}\sum_{j=1}^{N}\left(D_{i,j}(x,y)\right)^2 \quad \text{(C-26)}$$

where N denotes the level of decomposition and i takes values 1, 2, or 3, for the three detailed images of texture, and j is the wavelet coefficient index. More details on this method can be found in other references (*19*, *21*, *36*), Owing to the multi-resolution nature of the decomposition, the energy signature, or equivalently, the texture content has a physical meaning at each level. Energy signatures at higher levels reflect the "coarser" texture content of the sample, while those at lower levels reflect the "finer" texture content.

Direct Measurements of Particle Dimensions

Kuo and Freeman (*13*) proposed the texture parameter, which is expressed as follows:

$$\text{Texture Parameter} = \left(\frac{P}{P_{convex}}\right)^2 \quad \text{(C-27)}$$

Where, P is the perimeter of a particle measured on a black and white image, and P_{convex} is the perimeter of a bounding polygon.

REFERENCES

1. Barksdale, R. D., Kemp, M. A., Sheffield, W. J., and Hubbard. J. L. "Measurement of Aggregate Shape, Surface, Roughness." *Transportation Research Record 1301*, Transportation Research Board, National Research Council, Washington, D.C. (1991) pp.107-116.
2. Kuo, C. Y., Frost, J. D., Lai, J. S., and Wang, L. B. "Three-Dimensional Image Analysis of Aggregate Particle from Orthogonal Projections." *Transportation Research Record 1526*, Transportation Research Board, National Research Council, Washington, D.C. (1996) pp. 98-103.
3. Masad, E., Muhunthan, B., Shashidhar, N., and Harman T "Internal Structure Characterization of Asphalt Concrete Using Image Analysis." *ASCE Journal of Computing in Civil Engineering (Special Issue on Image Processing)*, Vol.13, No. 2 (1999a) pp. 88 – 95.
4. Masad, E. A., Muhunthan, B., Shashidhar, N., and Harman, T. "Effect of Compaction Procedure on the Aggregate Structure in Asphalt Concrete." *Transportation Research Record 1681*, Transportation Research Board, National Research Council, Washington, D.C. (1999b) pp. 179-184.
5. Brzezicki, J. M., and Kasperkiewicz, J. "Automatic Image Analysis in Evaluation of Aggregate Shape." *ASCE Journal of Computing in Civil Engineering (Special Issue on Image Processing),* Vol. 13, No. 2 (1999) pp. 123–130.

6. Weingart, R. L., and Prowell, B. D. "Specification Development Using the VDG-40 Videograder for Shape Classification of Aggregates." *Proceedings of the 7th Annual Symposium of the International Center for Aggregate Research (ICAR)*, University of Texas, Austin, TX (1999).
7. Maerz, N. H., and Zhou, W. "Flat And Elongated: Advances Using Digital Image Analysis." *Proceedings of the 9th Annual Symposium of the International Center for Aggregates Research (ICAR)*, Austin, TX (2001).
8. Tutumluer, E., Rao, C., and Stefanski, J. "Video Image Analysis of Aggregates." *Final Project Report, FHWA-IL-UI-278, Civil Engineering Studies UILU-ENG-2000-2015*, University of Illinois Urbana-Champaign, Urbana, IL (2000).
9. Li, L., Chan, P., Zollinger, D. G., and Lytton, R. L. "Quantitative Analysis of Aggregate Shape Based on Fractals." *ACI Materials Journal*, Vol. 90, No. 4 (1993) pp. 357-365.
10. Wilson, J. D., and Klotz, L. D. "Quantitative Analysis of Aggregates Based on Hough Transform." *Transportation Research Record 1530*, Transportation Research Board, National Research Council, Washington D.C. (1996) pp.111-115.
11. Yeggoni, M., Button, J. W., and Zollinger, D. G. "Influence of Coarse Aggregate Shape and Surface Texture on Rutting of Hot-Mix Concrete." *Texas Transportation Institute Report 1244-6*, Texas A&M University, College Station, TX (1994).
12. Masad, E., Button, J., and Papagiannakis, T. "Fine Aggregate Angularity: Automated Image Analysis Approach." *Transportation Research Record 1721,* Transportation Research Board, National Research Council, Washington D.C. (2000) pp.66–72.

13. Kuo, C., and Freeman, R. B. "Imaging Indices for Quantification of Shape, Angularity, and Surface Texture of Aggregates." *Transportation Research Record 1721*, Transportation Research Board, National Research Council, Washington D.C. (2000) pp. 57–65.
14. Masad, E. "Review of Imaging Techniques for Characterizing the Shape of Aggregates Used in Asphalt Mixes." *Proceedings of the 9th Annual Symposium of the* International Center for Aggregate Research (ICAR), Austin, TX (2001).
15. Rao, C., Tutumluer, E., and Kim, I. T. "Quantification of Coarse Aggregate Angularity Based on Image Analysis." *Transportation Research Record 1787*, Transportation Research Board, National Research Council, Washington, D.C. (2002) pp.117-124.
16. Hryciw, R. D., and Raschke, S. A. "Development of a Computer Vision Technique for In-Situ Soil Characterization." *Transportation Research Record 1526*, Transportation Research Board, National Research council, Washington, D.C. (1996) pp. 86-97.
17. Wang, L. B., and Lai, J. S. "Quantify Specific Surface Area of Aggregates Using an Imaging Technique." *Transportation Research Board 77th Annual Meeting*, Washington, D.C. (1998).
18. Masad, E., and Button, J. "Unified Imaging Approach for Measuring Aggregate Angularity and Texture." *Journal of Computer-Aided Civil and Infrastructure Engineering*, Vol. 15, No. 4 (2000) pp. 273-280.

19. Fletcher, T., Chandan, C., Masad, E., and Sivakumar, K. "Measurement of Aggregate Texture and Its Influence on HMA Permanent Deformation." *Journal of Testing and Evaluation, American Society for Testing and Materials, ASTM*, Vol. 30, No. 6, (2002) pp. 524-531.
20. Fletcher, T., Chandan, C., Masad, E., and Sivakumar, K. "Aggregate Imaging System (AIMS) for Characterizing the Shape of Fine and Coarse Aggregates." *Transportation Research Record 1832*, Transportation Research Board, National Research Council, Washington, D.C., (2003) pp. 67-77.
21. Chandan, C., Sivakumar, K., Fletcher, T., and Masad, E. "Geometry Analysis of Aggregate Particles Using Imaging Techniques." *Journal of Computing in Civil Engineering*, ASCE, Vol. 18, No. 1 (2004) pp. 75-82.
22. Fletcher, T. "Aggregate imaging System for Characterizing Fine and Coarse Aggregate Shape." Master's Thesis, Dept. of Civil and Environmental Engineering, Washington State University, Pullman, WA (2002).
23. Krumbein, W. C. "Measurement and Geological Significance of Shape and Roundness of Sedimentary Particles." *Journal of Sedimentary Petrology*, Vol. 11, No. 2 (1941) pp. 64-72.
24. Masad, E., Olcott, D., White, T., and Tashman, L. "Correlation of Fine Aggregate Imaging Shape Indices with Asphalt Mixture Performance." *Transportation Research Record 1757*. Transportation Research Board, National Research Council, Washington, D.C. (2001) pp. 148–156.

25. Wang, L. D., Park, J., and Mohammad, L. "Quantification of Morphology Characteristics of Aggregate from Profile Images." *Transportation Research Board 82nd Annual Meeting*, Washington, D.C. (2003).
26. Rosenfeld, A., and Kak, A. C. *Digital Picture Processing*, Academic Press, NewYork, NY (1976).
27. Blum, H. "A Transformation for Extracting New Descriptors of Shape." *Models for the Perception of Speech and Visual Form*, W. Wathen-Dunn, ed., M.I.T. Press, Cambridge, MA (1967) pp. 362-380.
28. Calabi, L., and Hartnett, W. E. "Shape Recognition, Particle Fires, Convex Deficiencies and Skeletons." *American Math Monthly*, Vol. 75, (1968) pp. 335-342.
29. Young, I. T., Peverini, R. L., Verbeek, P. W., and Van Otterloo, P. J. "A New Implementation for the Binary and Minkowski Operators." *Computer Graphics and Image Processing*, Vol. 17, No. 3 (1981) pp. 189-210.
30. Ehrlich, R., Kennedy, S. K., Crabtree, S. J., and Cannon, R. L. "Petrographic Image Analysis. I Analysis of Reservoir Pore Complexes." *Journal of Sedimentary Petrology*, Vol. 54, (1984) pp. 1365-1378.
31. Mandelbrot, B. B. *The Fractal Geometry of Nature*, W. H. Freeman, San Francisco, CA (1984).
32. Russ, J. C. *The Image Processing Handbook*, CRC Press LLC, Boca Raton, FL (1998).
33. Hough, P. "Methods and Means for Recognizing Complex Patterns." *U.S. Patent* Number 3,069,654, (1962).

34. Wilson, J. D., Klotz, L. D., and Nagaraj, C. "Automated Measurement of Aggregate Indices of Shape." *Particulate Science and Technology*, Vo. 15, (1997) pp. 13-35.

35. Maerz, N. H. "Technical and Computational Aspects of the Measurement of Aggregate Shape by Digital Image Analysis**."** *Journal of Computing in Civil Engineering*, Vol. 18, No. 1, (2004) pp. 10–18.

36. Mallat, Stephane G. "A Theory for Multiresolution Signal Decomposition: The Wavelet Representation." *IEEE Transactions on Pattern Analysis and Machine Intelligence*, Vol. 11, (1989) pp. 674-693.

APPENDIX D

TEST METHODS FOR MEASURING AGGREGATE CHARACTERISTICS

TEST METHODS FOR MEASURING AGGREGATE CHARACTERISTICS

Kandhal et al. (*1*), Janoo (*2*), and Chowdhury et al. (*3*) classified methods that are used to describe aggregate characteristics into two broad categories, namely, direct and indirect. Direct methods are defined as those wherein particle characteristics (shape, angularity, and texture) are measured, described qualitatively, and possibly quantified through direct measurement of individual particles. In indirect methods, particle characteristics are lumped together as geometric irregularities and determined based on measurements of bulk properties. Table D-1 shows a summary of direct and indirect test methods that have been used by highway state agencies and research projects for measuring some aspects of aggregate shape properties. The methods evaluated in this study include

In this appendix a brief description is provided for all test methods (direct and indirect) that are discussed in this report. It should be noted that when discussing a test method that has been selected for extensive evaluation, brief description of the testing procedures and modifications, if any, are reported too. It should be noted that, when discussing methods that were selected and evaluated in this study, the shape parameters obtained from each method are mentioned. These shape parameters have been presented and discussed in Appendix D. *The authors would like to bring the attention to the fact that some of the selected methods have been in practice for years, and they are usually performed using standard procedures. On the other hand, there are some methods that have been developed recently. For these methods, the manufacturer's or the developer's instructions were followed to perform the testing. It was necessary, in some cases, to perform the standard tests with minor modifications in order to conduct the tests on the selected aggregate sizes*.

Table D-1. Summary of Methods for Measuring Aggregate Characteristics

Test	References for the Test Method	Direct (D) or Indirect (I) Method	Field (F) or Central (C) Laboratory Application	Applicability to Fine (F) or Coarse (C) Aggregate
Uncompacted Void Content of Fine Aggregates	AASHTO T 304	I	F, C	F
Uncompacted Void Content of Coarse Aggregates	AASHTO TP 56, NCHRP Report 405, Ahlrich (*4*)	I	F, C	C
Index for Particle Shape and Texture	ASTM D3398	I	F, C	F, C
Compacted Aggregate Resistance	Report FHWA/IN/JTRP-98/20, Mr. David Jahn (Martin Marietta, Inc. personal communication)	I	F, C	F
Florida Bearing Ratio	Report FHWA/IN/JTRP-98/20, Indiana Test Method No. 201-89	I	F, C	F
Rugosity	Tons and Goetz (*5*), Ishai and Tons (*6*)	I	F, C	F
Time Index	Quebec Ministry of Transportation , Janoo (*2*)	I	F, C	F
Angle of Internal Friction from Direct Shear Test	Chowdhury et al. (*3*)	I	C	F, C
Percentage of Fractured Particles in Coarse Aggregate	ASTM D 5821	D	F, C	C
Flat and Elongated Coarse Aggregates	ASTM D 4791	D	F, C	C
Multiple Ratio Shape Analysis	Mr. David Jahn (Martin Marietta, Inc.)	D	F, C	C
VDG-40 Videograder	Emaco, Ltd. (Canada), Weingart and Prowell (*7*)	D	F, C	F, C
Computer Particle Analyzer	Mr. Reckart (W.S. Tyler Mentor Inc.), Tyler (*8*)	D	C	F, C
Micromeritics OptiSizer (PSDA)	Mr. M. Strickland (Micromeritics OptiSizer)	D	C	F, C
Video Imaging System (VIS)	John B. Long Company	D	C	F, C
Buffalo Wire Works (PSSDA)	Dr. Penumadu, University of Tennessee	D	C	F, C
Camsizer	Jenoptik Laser Optik System and Research Technology	D	C	F,C
WipShape	Maerz and Zhou (*9*)	D	C	C
University of Illinois Aggregate Image Analyzer (UIAIA)	Tutumluer et al. (*10*), Rao (*11*)	D	C	C
Aggregate Imaging System (AIMS)	Masad (*12*)	D	C	F, C
Laser-Based Aggregate Analysis System	Kim et al., (*13*)	D	C	C

Note: AASHTO = American Association of State Highway and Transportation Officials; FHWA= Federal Highway Administration; JTRP = Joint Transportation Research Program; ASTM = American Society of Testing and Materials.

Indirect Methods

As defined earlier, indirect test methods are those methods in which particle characteristics are lumped together as geometric irregularities and determined based on measurements of bulk properties. In indirect methods, the shape, angularity, and texture are usually combined, as it is fairly difficult to separate the effect of the individual components. A brief discussion is provided below about the commonly used indirect methods.

**AASHTO T 304 (ASTM C 1252) Uncompacted Void Content of Fine Aggregate*

The Uncompacted Void Content of Fine Aggregate was originally developed by the National Aggregate Association (NAA) and was later adopted by the American Society for Testing and Material (ASTM) as method C 1252 (*14*) and by the American Association of State Highway and Transportation Officials (AASHTO) (as method T 304 (*15*). This method is often referred to as the Fine Aggregate Angularity (FAA) test. It measures the loose uncompacted void content of a sample of fine aggregate that falls from a fixed distance through a given-sized orifice. A decrease in the void content is associated with more rounded, spherical, smooth-surface fine aggregate or a combination of these factors. Method A of this procedure is used by Superpave to determine aggregate angularity to ensure that fine aggregate has adequate internal friction to provide rut resistance to an HMA. This method has been extensively evaluated in a number of studies (*2, 16, 17, 18, 19, 20, 21*). The apparatus used in this test method is shown in Figure D-1.

This test was conducted at the Texas Transportation Institute (TTI). Method B of this test procedure was performed, where individual size fractions are tested using the smaller two sizes

Figure D-1. Uncompacted Void Content of Fine Aggregate Apparatus.

of the proposed fine aggregate sizes: 2.36 - 1.18 mm (sieve #8 - #16) and 0.6 - 0.3 mm (sieve #30 - #50). The size of 4.75 - 2.36 mm (sieve #4 - #8) was not tested for two reasons: First, this size was not included in the specifications, and second, this aggregate particles size did not pass through the orifice of the test apparatus freely. Complying with the standards, a 190 g sample size was used. In this study, the results are reported using the individual sizes, a slight modification from the Method B procedure, which requires that the average uncompacted void content from the three sizes to be reported.

**AASHTO TP 56 Uncompacted Void Content of Coarse Aggregate*

This method was originally developed by the NAA and was later adopted by AASHTO as method TP 56. It measures the loose uncompacted void content of a sample of coarse aggregate that falls from a fixed distance through a given-sized orifice. A decrease in the void content is associated with more rounded, spherical, smooth-surface coarse aggregate or a combination of these factors. Method A of this procedure is used by Superpave to determine aggregate angularity. This method was evaluated in a number of studies (*4, 18, 20*). The apparatus used in this method is shown in Figure D-2.

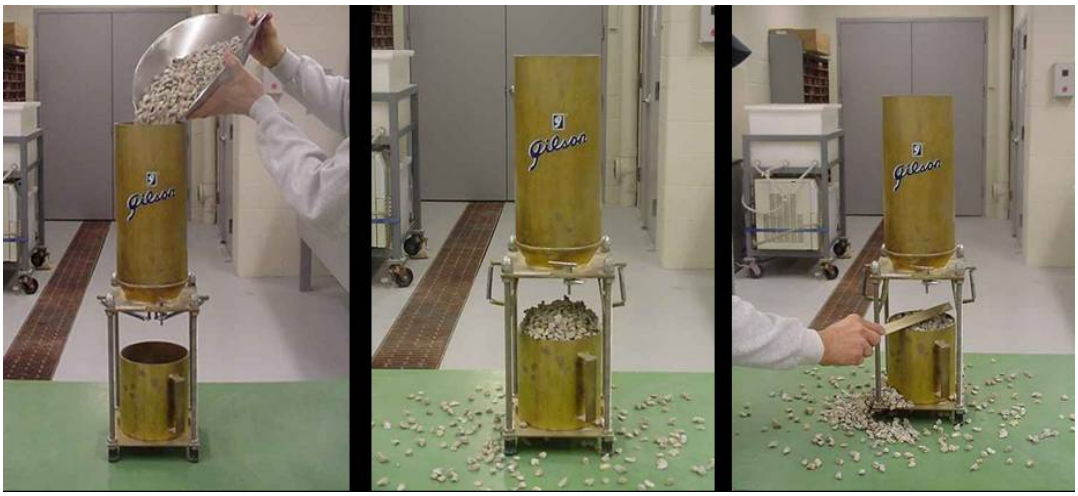

Figure D-2. Uncompacted Void Content of Coarse Aggregate Apparatus.

This test was conducted at TTI. Method B of this test procedure was performed, where individual size fractions are tested. This test was conducted on coarse aggregate sizes 12.5 – 9.5 mm (1/2 - 3/8 inches) and 9.5 – 4.75 mm (3/8"- #4). A sample size of 5000 g was used. In this study, the results are reported using the individual sizes, a slight modification from the Method B procedure, which requires that the average uncompacted void content from the three sizes to be reported.

ASTM D 3398 Standard Test Method for Index of Aggregate Particle Shape and Texture

This test provides an index of an aggregate sample as an overall measure of its shape and texture. The test is based on the concept that not only shape, angularity, and texture of uniformly sized aggregate affects void ratio, but also the rate at which the voids change when compacted in a standard mold (*14, 17, 22, 23*).

**Compacted Aggregate Resistance (CAR) Test*

The CAR test was developed by Mr. David Jahn for evaluating shear resistance of compacted fine aggregate in its as-received condition. The test works by applying a compressive load on the aggregate specimen using the Marshall testing machine. The compressive load versus displacement is plotted. The maximum compressive load that the specimen can carry is reported as CAR stability value. This value is assumed to be a function of the material shear strength and angularity. The CAR test method has many similarities with California Bearing Ratio test (*16, 20, 23*). Figures D-3 shows the CAR testing setup.

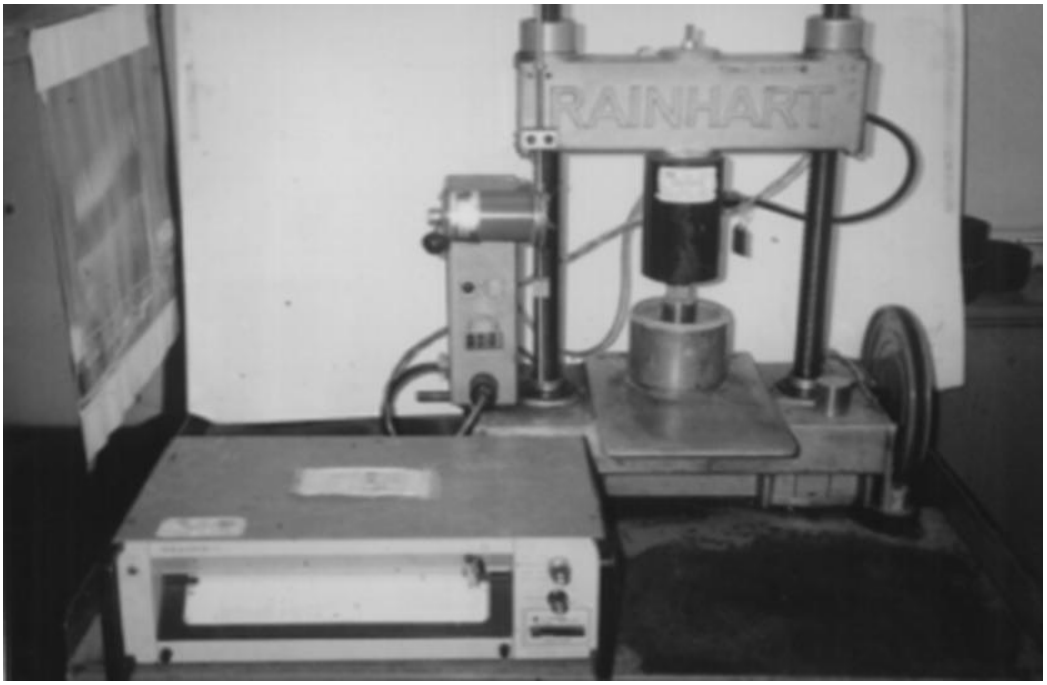

Figure D-3. CAR Testing Machine.

The CAR test was conducted at TTI with some modifications to the procedure provided by Mr. David Jahn. The procedure suggested by Mr. Jahn was to use the fine aggregates of a job-mix-blend used in the preparation of the asphalt mix in their as-blended condition. Two options were available. The first was to test the individual aggregate sizes. This option was dismissed after consultation with Mr. Jahn since these individual particles would not have the shear resistance that would develop from using combined sizes. The second option, which was followed in this study, was to develop a blend using the three fine aggregate sizes used in this study. The blend used here is given in Table D-2. The sample size was 1200 g. The aggregate sample was oven-dried, and then 3.5 percent moisture was added to the specimen. The sample was placed in a mold, and 50 blows were applied on one face only. The sample was then placed in the Marshall stability machine and tested at 2 inch/min to report shear resistance versus penetration. The test provides information on the shear resistance of compacted fine aggregates (CAR) which is used as a measure of angularity. Higher shear resistance is associated with higher angularity.

Florida Bearing Ratio

This test method is used to determine the Florida Bearing value for fine aggregates used in HMA. The basic concept for this method is to determine the deformation rate of a fine aggregate subjected to a constant rate of loading. This deformation rate is taken as an indirect measure of angularity (*23, 24*). Figure D-4 shows a schematic description of Florida Bearing ratio apparatus.

Table D-2 Fine Aggregate Blend Used in CAR Test

Size	Percentage
4.75 – 2.36 mm (sieve #4-#8)	40%
2.36 – 1.18 mm (sieve #8-#16)	20%
0.6 – 0.3 mm (sieve #30-#60)	40%

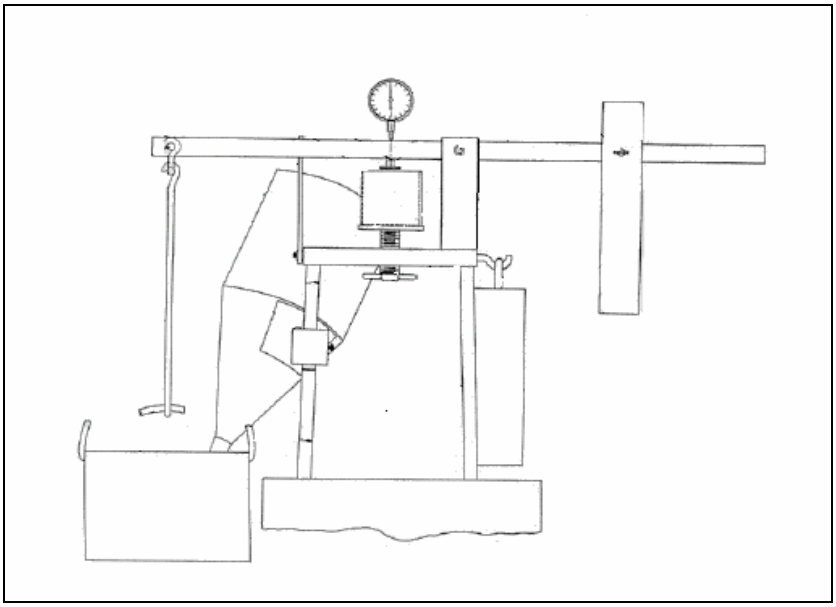

Figure D-4. Schematic Description of Florida Bearing Ratio Apparatus Florida Bearing Value of Fine Aggregate (Indiana State Highway Commission Method 201).

Rugosity

This method was first developed by Tons and Goetz (*5*) for coarse and fine aggregates. The method is based on relating the flow rate of aggregates through a given-sized orifice to their shape properties (2, 5, 6, 17). Schematic description of the pouring device as presented by Janoo (*2*) is shown in Figure D-5.

Time Index

This test method was developed in France in 1981, and Quebec Ministry of Transportation Aggregate Laboratory in Quebec City uses this test. It was used for fine aggregates only, but it can be modified to measure the properties of coarse aggregates. Similar to the rugosity test, the basis for this method is that the flow rate of an aggregate mass through a known orifice is affected by angularity, surface texture, and bulk specific gravity of the aggregate (*2, 17*). Time Index test apparatus is shown in Figure D-6.

AASHTO T 236 (ASTM D 3080) Direct Shear Test

This test is normally conducted in accordance with the AASHTO T 236 or ASTM D 3080 procedure. This test is used to measure the internal friction angle of a fine aggregate under different normal stress conditions. A prepared sample of the aggregate is consolidated in a shear mold. The sample is then placed in a shear device and sheared by a horizontal force while a normal stress is applied (*16, 23*). Figure D-7 shows the direct shear testing machine.

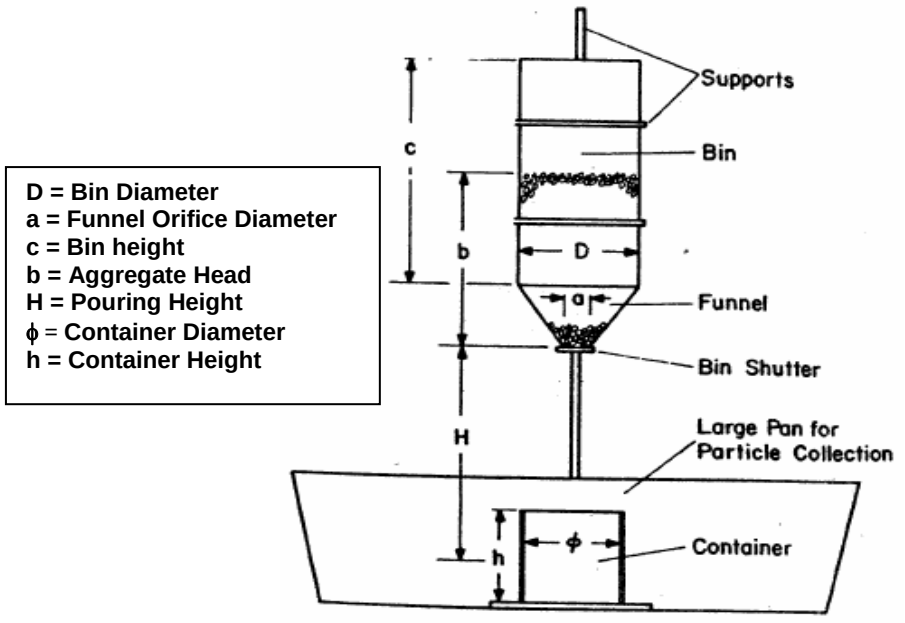

Figure D-5. Schematic Description of the Pouring Device Used by Rugosity Test.

Figure D-6. Time Index Test Apparatus.

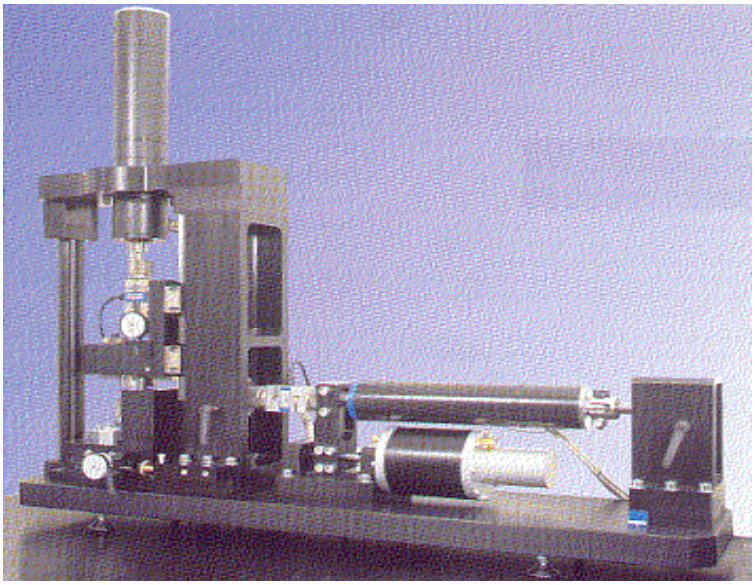

Figure D-7. Direct Shear Testing Machine.

Direct Methods

These methods vary in the level of sophistication used to obtain direct information on aggregate shape. For example, the ASTM D 5821 procedure simply relies on visual inspection of aggregates, and ASTM D 4791 uses a mechanical device to classify aggregates according to the proportions of aggregate dimensions. The method developed by Jahn (*25*) uses a digital caliper to provide the distribution of the proportions of aggregate dimensions, and the rest of the direct methods use imaging systems and analysis procedures to measure aggregate dimensions. An imaging system consists of a mechanism for capturing images of aggregates and methods for analyzing aggregate characteristics. Table D-1 summarizes the majority of the imaging systems available commercially or in research institutions.

In addition to the systems in Table D-1, several studies have presented experimental setups to facilitate capturing aggregate images (*26, 27, 28)*. Imaging systems and analysis procedures focus on quantifying shape or form (*7, 9, 10, 26, 28, 29, 30, 31)*, angularity (*27, 32, 33, 34, 35, 36, 37*, and texture (*27, 38, 39, 40*).

**ASTM D 5821 Determining the Percentages of Fractured Particles in Coarse Aggregate*

Determining the percentages of fractured particles in coarse aggregate test method is considered to be a direct method for measuring coarse aggregate angularity. The method is based on evaluating the angularity of an aggregate sample (mostly used for gravel) by visually examining each particle and counting the number of crushed faces, as illustrated in Figure D-8. It is also the method currently used in the Superpave system for evaluating the angularity of coarse aggregate used in HMA (*19, 20, 21*).

In this test method, which was conducted at TTI, the size of the sample was chosen such that the number of particles exceeded 50 for aggregate sizes 25.4 – 19.0 mm (1- 3/4 inches) and

Figure D-8. Illustration of Counting Percent of Fractured Faces.

12.5 – 9.5 mm (1/2 - 3/8 inches). For the smaller size of 9.5 – 4.75 mm (3/8"- #4) a sample size of 200 grams, as recommended by specifications, was used. The total sample weight from each aggregate type always exceeded 500 g, as specified by ASTM D5821. This method provides information on the angularity of coarse aggregate by visually examining each particle and counting the number of fractured or crushed faces (PFF). A high percent of crushed faces (one face, two or more faces) is associated with higher angularity.

**ASTM D 4791 Flat and Elongated Coarse Aggregates*

Flat and Elongated Coarse aggregate method provides the percentage by number or weight of flat, elongated, or both flat and elongated particles in a given sample of coarse aggregate. The procedure uses a proportional caliper device, as shown in Figure D-9, to measure the dimensional ratio of aggregates. The aggregates are classified according to the undesirable ratios of width to thickness or length to width, respectively. Superpave specifications characterize an aggregate particle by comparing its length to its thickness or the maximum dimension to the minimum one (*20, 21, 22, 41, 42*) .

This test method was also conducted at TTI. The test specification does not provide a procedure for testing samples of one size. Researchers decided to use the same aggregate sample size that was used in conducting ASTM D5821. This method provides the percentage by number or weight of flat, elongated, or both flat and elongated particles in a given sample of coarse aggregates. Following Superpave specifications, the ratios of length to thickness or the maximum dimension to the minimum dimension were reported in this study (FER).

Figure D-9. Flat and Elongated Coarse Aggregate Caliper.

**Multiple Ratio Shape Analysis (MRA)*

MRA test method was developed by Mr. David Jahn (*25*). The method is used for categorizing various particle shapes found in a coarse aggregate sample. It is based on classifying aggregates according to their dimensional ratios into five different categories instead of one (<2:1, 2:1 to 3:1, 3:1 to 4:1, 4:1 to 5:1, >5:1). The device consists mainly of a digital caliper connected to a data acquisition system and a computer. A particle is placed on a press table, and the press is lowered until it touches the aggregate particle and stops. The device records the gap between the press and the table, which is equal to the particle dimension. The particle is then rotated in another direction and the procedure is repeated to obtain other dimensions. These readings are recorded in a custom designed spreadsheet that displays the distribution of dimensional ratio in the aggregate sample (*25*). Figure D-10 shows the digital MRA device.

This test was conducted at TTI. In this method, aggregates were classified according to their dimensional ratios into five different categories instead of one (<2:1, 2:1 to 3:1, 3:1 to 4:1, 4:1 to 5:1, >5:1). There was no specific sample size, as there were no standards for this test; therefore, it was decided, after consulting with Mr. David Jahn, that the same samples and sample sizes that were used in the flat and the elongated test and fractured faces test be used in this test.

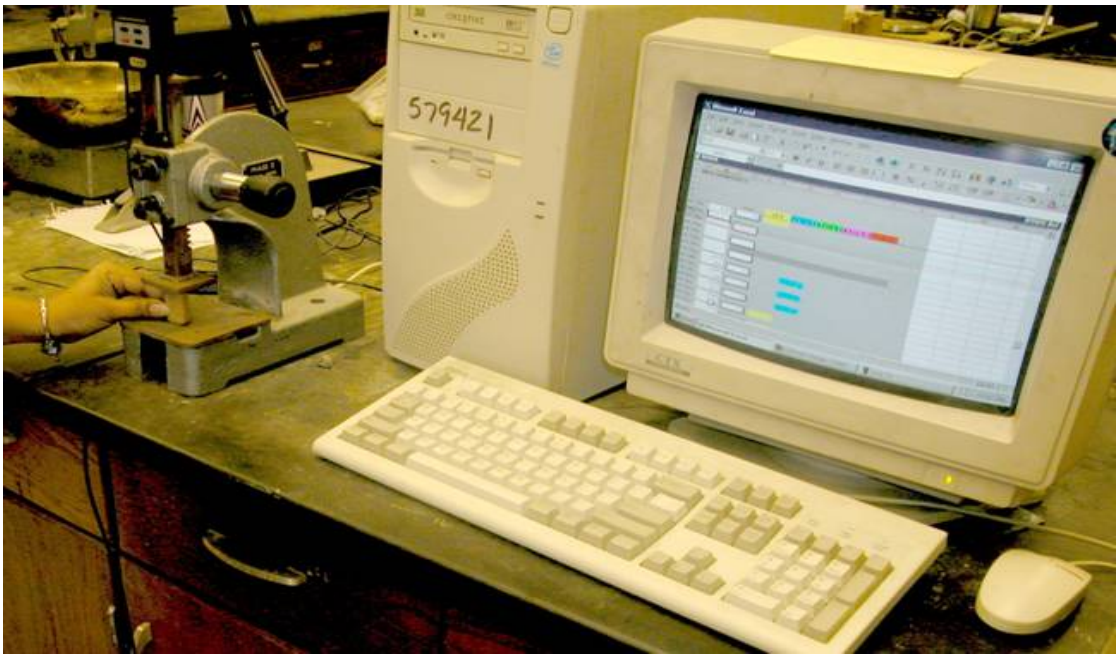

Figure D-10. Improved Digital Multiple Ratio Analysis Device (MRA) by Martin Marietta.

**VDG-40 Videograder*

VDG-40 Videograder was developed by the French public works laboratory (LCPC). In this system, an electromagnetic vibrator extracts the constituents of the sample in the hopper and directs them a long a feed channel toward separator drums. The separator drum orients the aggregates toward the falling plane at the required speed. The system uses a line-scan CCD camera to image and evaluate particles as they fall in front of the backlight. A mathematical procedure based on assuming elliptical particles is used to calculate each particle's third dimension from the two-dimensional (2-D) projection images captured. All analysis and data reporting are performed in a custom software package. This system is used in the laboratory to obtain automated aggregate gradation measurements and also particle flatness (VDG-40 FLAT) and slenderness ratios (VDG-40 SLEND) (*43, 44*). Figures D-11(a) and D-11(b) show, respectively, the VGD-40 Videograder and a schematic of image acquisition of falling aggregates.

The VDG-40 Videograder was brought from Turner-Fairbank Highway Research Center to the TTI where coarse aggregate testing was conducted. The VDG 40 Videograder has no standard specification for sample size. Researchers decided to use a 1.0-kg sample size to ensure that the sample will contain at least 50 particles, which is considered a statistically valid number.

Computer Particle Analyzer CPA

The Computer Particle Analyzer (CPA) is similar to the VDG-40 Videograder, as it uses a line-scan CCD camera to image and evaluate every particle in the sample as it falls in front of the backlight. However, it can be used in the laboratory as well as on-line (continuous scanning of a product stream). The current analysis of this system focuses on gradation and shape by assuming an idealized shape for aggregate particles to obtain the third dimension from images of

(a)

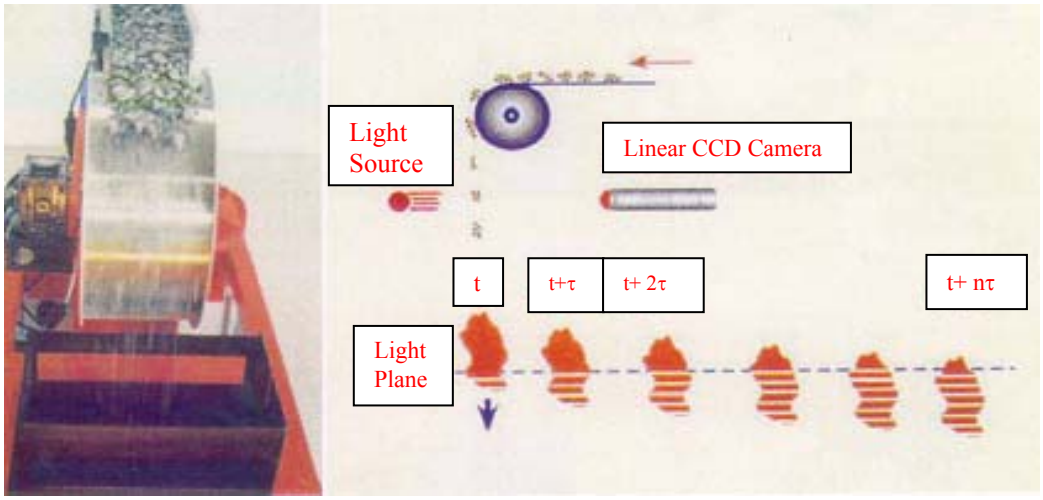

(b)

Figure D-11. VDG-40 Videograder. (a) Components of VDG-40 Videograder and (b) Image Acquisition of Falling Aggregates in VDG 40 Videograder.

2-D projection. All analysis and data reporting are performed in a custom software package (*8, 43*). CPA system and a schematic description of the CPA are shown in Figures D-12(a) and D-12(b), respectively.

Micromeritics OptiSizer (PSDA)

This device was initially developed for online applications. The system uses a line-scan CCD camera to image and evaluate particles in a sample as it falls in front of the backlight. Similar to the image analysis system discussed above, an idealized shape of particles is used to provide information about gradation and shape. All analysis and data reporting are performed in a custom software package (*43*). Figure D-13 shows the Micromeritics OptiSizer PSDA system.

Video Imaging System (VIS)

This system uses a line-scan CCD camera to image and evaluate particles in the sample as it falls in front of the backlight. Similar to the VDG-40 Videograder system, VIS assumes an idealized shape of a particle to provide information on gradation and shape. All analysis and data reporting are performed in a custom software package (*43*). The VIS is shown in Figure D 14.

(a)

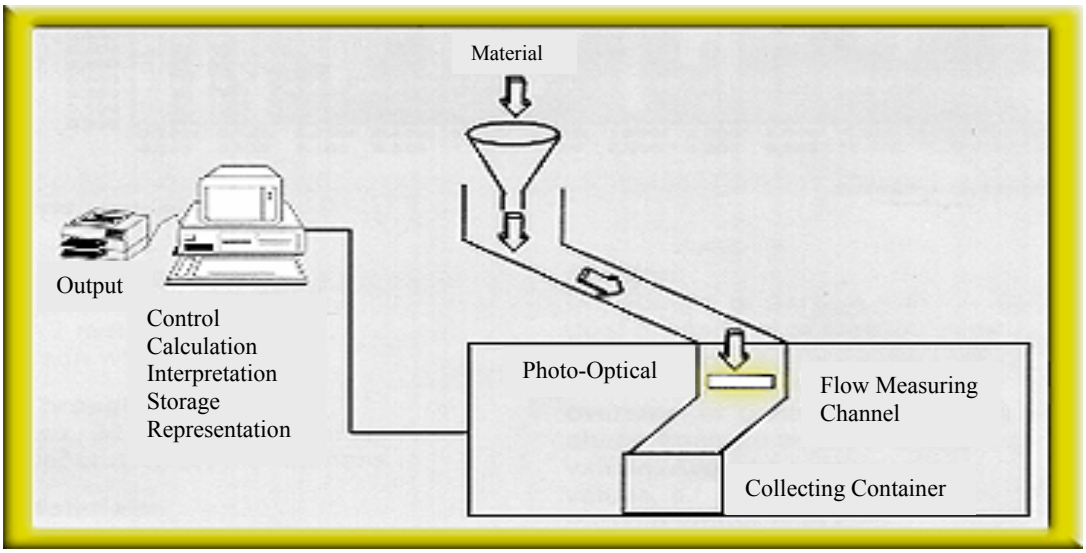

(b)

Figure D-12. Computer Particle Analyzer System (CPA). (a) Components of Computer Particle Analyzer System (CPA) and (b) Schematic Description of How CPA Works.

Figure D-13. Micromeritics OptiSizer (PSDA).

Figure D-14. Video Imaging System (VIS).

**Buffalo Wire Works (PSSDA)*

Buffalo Wire Works (PSSDA) system was developed by Dr. Dayakar Penumadu, currently with the University of Tennessee. The system captures images of particles as they fall in front of the backlight. The system, mainly developed for a laboratory environment, provides information about gradation and shape. All analysis and data reporting are performed in a custom software package (*43*). Dr. Dayakar Penumadu created two experimental test devices that have the same analysis concept. These devices are called PSSDA-Large and PSSDA-Small. PSSDA-Large is devoted to analyzing coarse aggregate particles while PSSDA-Small is used for analysis of fine aggregates. Figure D-15 shows both.

This test was performed at the University of Tennessee. Similar to the principle of the VDG-40 Videograder and Camsizer, the system uses one line-scan CCD camera to image and evaluate particles as they fall in front of the backlight. The test method was conducted using a 1.0-kg coarse aggregate sample and a 0.50-kg fine aggregate sample. The system provides information about gradation and shape. Roundness (ROUND), which is defined in Appendix D, is used to describe shape.

(a)

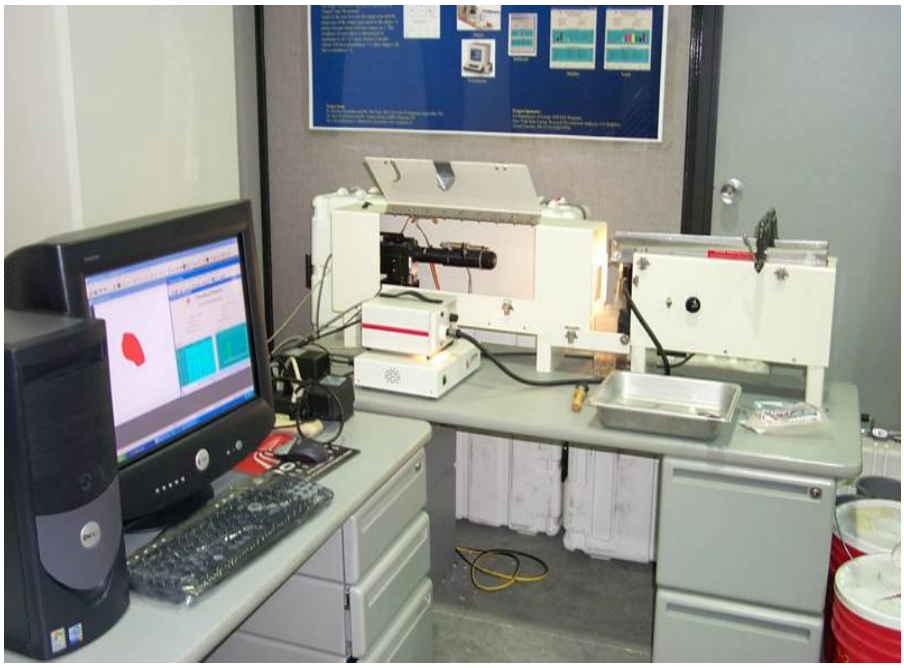

(b)

Figure D-15. Buffalo Wire Works (PSSDA) Systems for Coarse and Fine Aggregates. (a) PSSDA-Large and (b) PSSDA-Small.

**Camsizer*

Two optically matched digital cameras comprise the heart of the Camsizer system as seen in Figure D-16(a). These two cameras are used to capture images of fine and coarse aggregates at different resolutions. Individual particles exit the hopper to a vibrating feed channel and fall between the light source and the camera. Particles are detected as projected surfaces and digitized in the computer. This commercially available system automatically produces particle size distributions and some aspects of particle characteristics (Christison Scientific Equipment Ltd). Figure D-16(b) shows an illustration of the Camsizer.

This test was conducted at TTI. The system was not capable of analyzing the large size of coarse aggregates 25.4 – 19.0 mm (1 - 3/4 inches), since these aggregates were too large to pass through the hopper. The Camsizer measures the following parameters: Aggregate form, sphericity (CAMSPHT), symmetry (CAMSYMM), and length to breadth (CAML/B); Angularity in the Camsizer is described using convexity (CAMCONV). These parameters are described in Appendix C. The test was conducted using a 1.0-kg sample size of coarse aggregates and about 200 grams of fine aggregates.

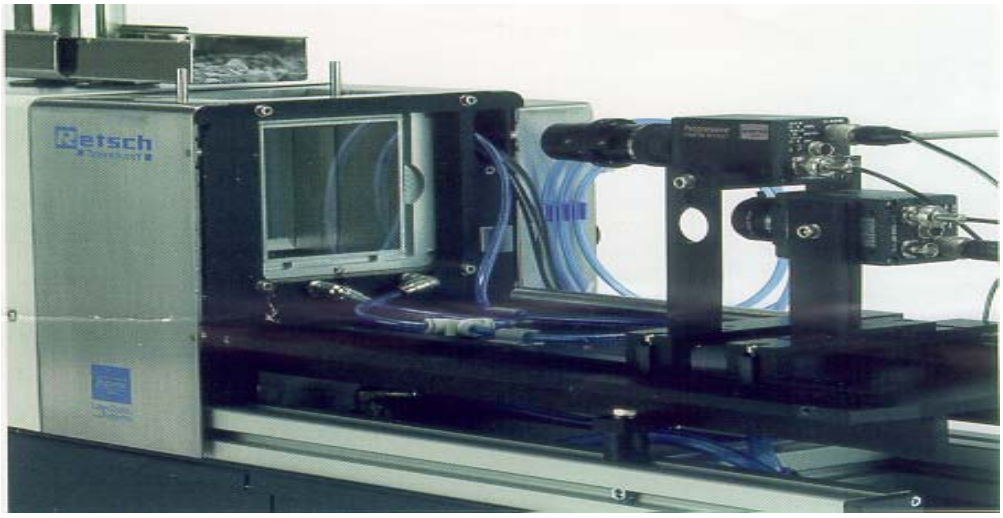

(a)

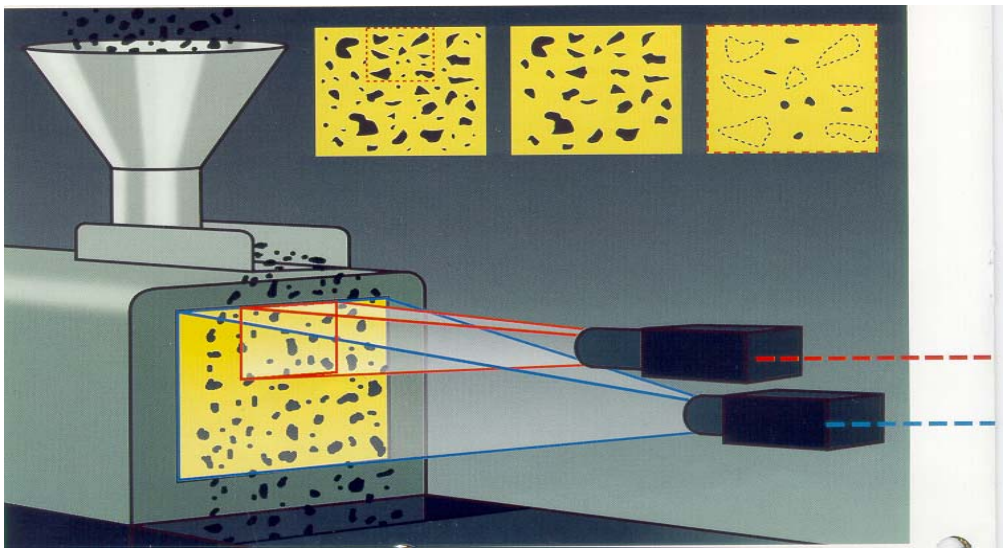

(b)

Figure D-16. Camsizer System. (a) Overall View of the Camsizer and (b) Illustration of the Two Cameras Used in the Camsizer.

**WipShape*

The system was developed by Dr. Maerz at the University of Missouri for coarse aggregate analysis. In the first version of the system, the aggregate particles were fed from a hopper into a mini-conveyor system. In a more recent version, the aggregate particles are placed in front of two orthogonal oriented synchronized cameras, which capture images of each particle from two views. These images are used to determine the three dimensions of particles. The system provides information on aggregate shape and gradation (*9, 44, 45*). Figure D-17 below shows the most recent version of WipShape System.

This test was conducted at the University of Illinois. WipShape provides a measure of aggregate shape by providing information on the dimensional ratio from particle images (WSFER). WipShape uses the minimum average curve radius method, described in Appendix D, to quantify aggregates angularity (WSMACR).

**University of Illinois Aggregate Image Analyzer (UIAIA)*

This method was selected and evaluated in this study. UIAIA was developed by Dr. Tutumluer with the University of Illinois. It uses three cameras to capture projections of coarse particles as they move on a conveyer belt. These projections are used to reconstruct three-dimensional representations of particles. The shape is determined from the measured dimensions directly without the need to assume idealized shape of particles. The system provides information on gradation, shape, angularity, and texture (*46*). The UIAIA and the aggregate detection system are shown in Figures D-18(a) and D-18(b), respectively.

Figure D-17. WipShape System .

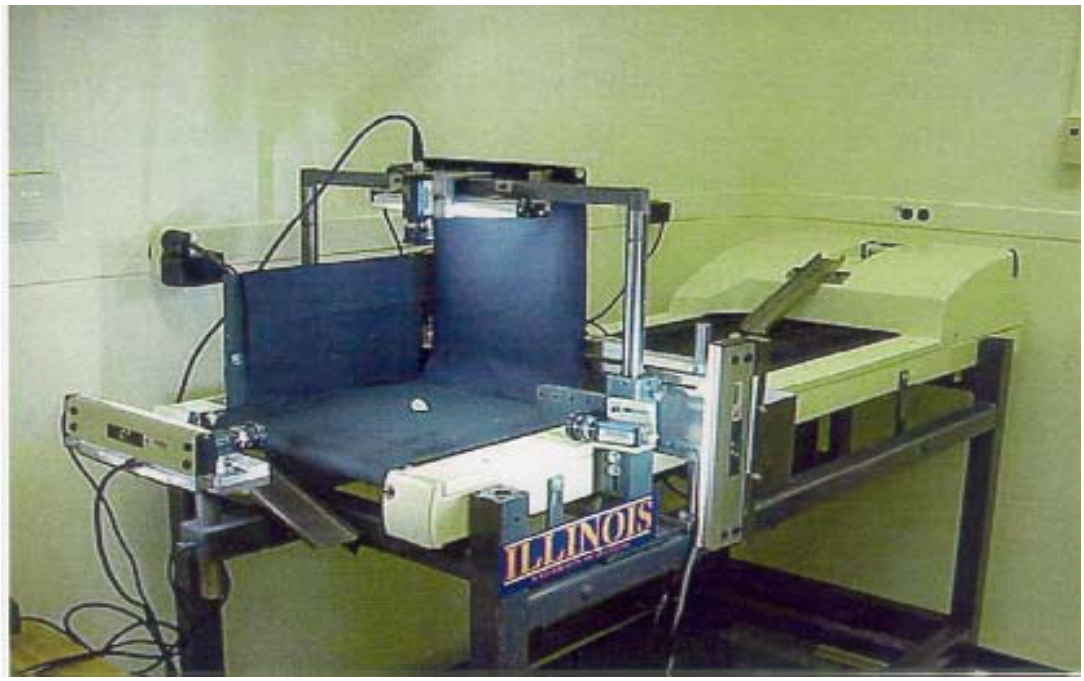

(a)

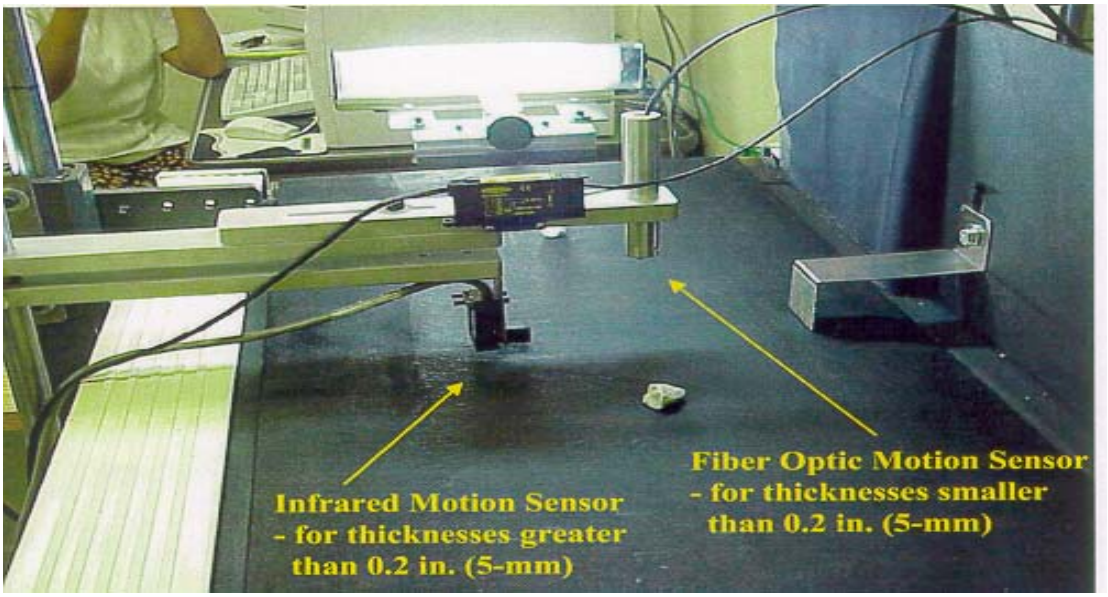

(b)

Figure D-18. University of Illinois Aggregate Image Analyzer (UIAIA). (a) Components of the UIAIA System and (b) Details of the Aggregate Detection System.

This method was conducted at the University of Illinois. Particles are placed individually on the conveyer belt. Once a particle is detected at a certain location on the conveyer belt using sensors, the cameras capture the three projections of particles individually. Some of the aggregates with dark color were not measured using this system. The UIAIA measures all three aggregate characteristics (shape, angularity, and texture). The methods used by UIAIA to measure these properties were presented in Appendix C. Shape of aggregate particles is measured by calculating the flat and elongated ratio (UIFER). The UIAIA measures angularity (UIAI) using the outline slope method, while aggregate surface texture (UISTI) is measured using the erosion-dilation method.

**Aggregate Imaging System (AIMS)*

This system was developed by Dr. Eyad Masad. The system operates based on two modules. The first module is for the analysis of fine aggregates; black and white images are captured using a video camera and a microscope. The second module is devoted to the analysis of coarse aggregate; gray images as well as black and white images are captured. Fine aggregates are analyzed for shape and angularity, while coarse aggregates are analyzed for shape, angularity, and texture. The video microscope is used to determine the depth of particles, while the images of 2-D projections provide the other two dimensions. These three dimensions quantify shape. Angularity is determined by analyzing the black and white images, while texture is determined by analyzing the gray images (*12, 47*). AIMS is shown in Figure D-19.

AIMS tests were conducted at TTI. AIMS uses 56 particles when analyzing coarse aggregates and few grams when analyzing fine aggregates. The system analyzes all aggregate

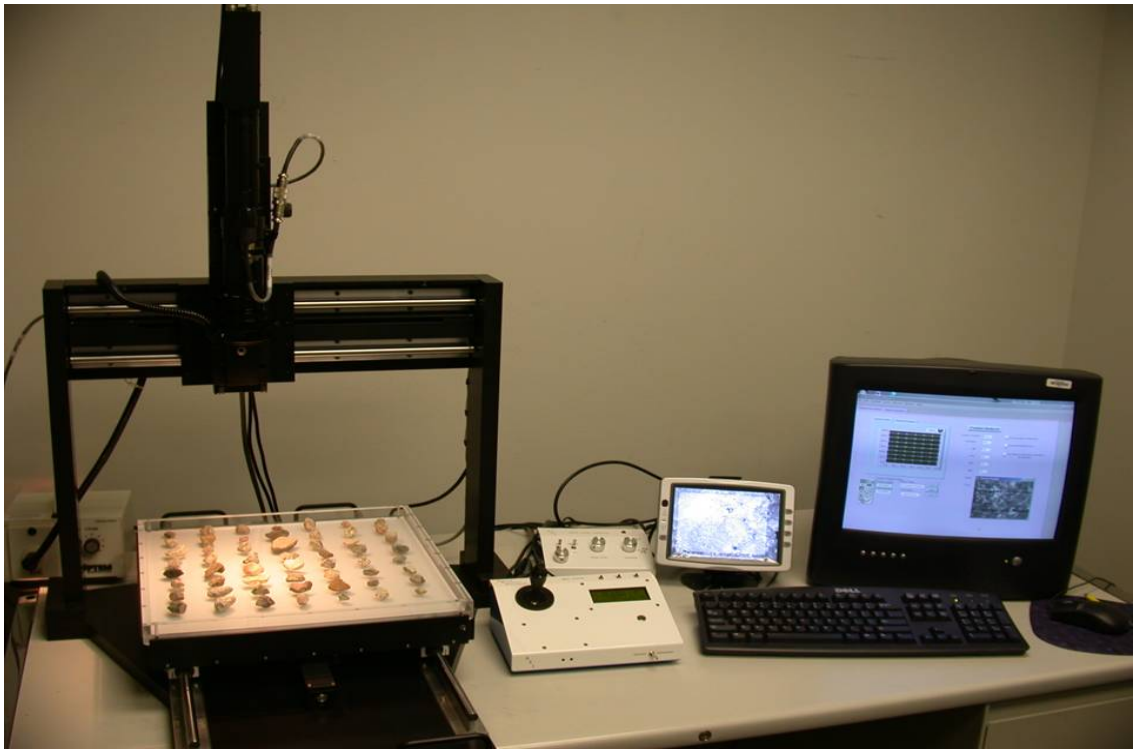

Figure D-19. Aggregate Imaging System (AIMS).

sizes (coarse and fine) and provide the following measures for aggregate shape: Sphericity (AIMSSPH) and dimensional ratio for coarse aggregates and 2-D form index (AIMSFORM) for fine aggregates; angularity: gradient angularity index (AIMSGRAD) and radius angularity index (AIMS RAD); and texture: texture index (wavelet) (AIMSTXTR). A description of all these parameters is provided in Appendix C.

**Laser-Based Aggregate Analysis System (LASS)*

This system was initially selected for evaluation but it was not made available to this study during the experimental evaluation period. LASS was developed by Dr. Carl Hass and Dr. Alan Rauch at the University of Texas-Austin to characterize size and shape parameters of coarse aggregates. A laser scanner is mounted on a linear motion slide that passes over an sample aggregate scattered on a flat platform, scanning the particles using a vertical laser plane. The 3-D scanner data are transformed into gray-scale digital images, where the gray scale pixel values present the height of each datum point. These heights are used to calculate aggregate characteristics. These images are used to determine parameters of shape, angularity, and texture (*13, 48*). Figure D-20 shows a schematic description of LASS.

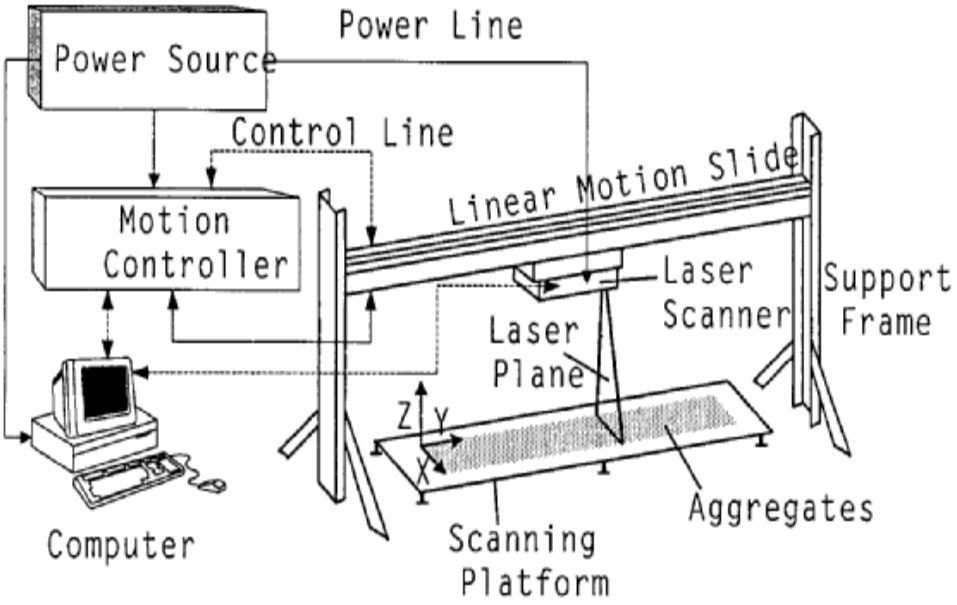

Figure D-20. Laser-Based Aggregate Scanning System (LASS) Hardware Architecture.

REFERENCES

1. Kandhal, P. S., Motter, J. B., and Khatri, M. A. "Evaluation of Particle Shape and Texture: Manufactured Versus Natural Sands." *Transportation Research Record 1301*, Transportation Research Board, National Research Council, Washington D.C. (1991) pp. 48-67.
2. Janoo, V. C. "Quantification of Shape, Angularity, and Surface Texture of Base Course Materials." *U.S. Army Corps of Engineers Special Report 98-1*, Cold Regions Research & Engineering Laboratory, Hanover, NH (1998).
3. Chowdhury, A., Button, J. W., Kohale, V., and Jahn, D. "Evaluation of Superpave Fine Aggregate Angularity Specification." *International Center for Aggregates Research ICAR Report 201-1*, Texas Transportation Institute, TX (2001).
4. Ahlrich, R. C. "Influence of Aggregate Gradation and Particle Shape/Texture on Permanent Deformation of Hot-Mix Asphalt Pavement." Ph.D. Dissertation., Auburn University. Auburn, AL (1995).
5. Tons, E., and Goetz, W. H. "Packing Volume Concepts for Aggregates." Highway *Research Record* 236, Transportation Research Board, National Research Council, Washington D.C. (1968) pp. 79-96.
6. Ishai, I., and Tons, E. "Concept and Test Methods for a Unified Characterization of the Geometric Irregularity of Aggregate Particles." *Journal of Testing and Evaluation*, Vol. 5, No. 1 (1977) pp. 3-15.

7. Weingart, R. L., and Prowell, B. D. "Specification Development Using the VDG-40 Videograder for Shape Classification of Aggregates." *Proceedings of the 7th Annual Symposium of the International Center for Aggregate Research (ICAR)*, University of Texas, Austin, TX (1999).
8. Tyler, W. S. "*Particle Size and Shape Analyzers (CPA*)." Product Brochure, Mentor, OH (2001).
9. Maerz, N. H., and Zhou, W. "Flat and Elongated: Advances Using Digital Image Analysis." *Proceedings of the 9th Annual Symposium of the International Center for Aggregates Research (ICAR)*, Austin, TX (2001).
10. Tutumluer, E., Rao, C., and Stefanski, J. "Video Image Analysis of Aggregates." *Final Project Report, FHWA-IL-UI-278, Civil Engineering Studies UILU-ENG-2000-2015*, University of Illinois Urbana-Champaign, Urbana, IL (2000).
11. Rao, C. "Development of 3-D Image Analysis Techniques to Determine Shape and Size Properties of Coarse Aggregate." Ph.D. Dissertation, Dept. of Civil Engineering, University of Illinois at Urbana-Champaign, Urbana, IL (2001).
12. Masad, E. "The Development of a Computer Controlled Image Analysis System for Measuring Aggregate Shape Properties." *National Cooperative Highway Research Program NCHRP-IDEA Project 77 Final Report*, Transportation Research Board, National Research Council, Washington, D.C (2003).

13. Kim, H., Haas, C., Rauch, A., and Browne, C. "A Prototype Laser Scanner for Characterizing Size and Shape Properties in Aggregates." *Proceedings of the 9th Annual Symposium of the International Center for Aggregate Research (ICAR)*, Austin, TX (2001).
14. American Society of Testing and Materials ASTM. *Annual Book of ASTM Standards (03-04)*, West Conshohocken, PA (2000).
15. American Association of State Highway and Transportation Officials AASHTO. *Standard Specifications for Transportation Materials and Methods of Sampling and Testing*, 19th Edition, Washington, D.C (1988).
16. Chowdhury A., and Button, J. W. "Fine Aggregate Angularity: Conventional and Unconventional Approach, Aggregate Contribution to Hot-Mix Asphalt HMA Performance." *American Society for Testing and Materials ASTM, Special Technical* Publication, Vol. 1412, (2001) pp. 144-159.
17. Janoo, V. C., and Korhonen, C. "Performance Testing of Hot-Mix Asphalt Aggregates." *U.S. Army Corps of Engineers Special Report 99-20*, Cold Regions Research & Engineering Laboratory, Hanover, NH (1999).
18. Kandhal, P. S., and Parker, F. Jr. "Aggregate Tests Related to Asphalt Concrete Performance in Pavements." *National Cooperative Highway Research Program Report 405*, Transportation Research Board, National Research Council, Washington, D.C (1998).

19. Lee, J. C., Changlin, P., and White, T. "Review of Fine Aggregate Angularity Requirements in Superpave." *Journal of the Association of Asphalt Paving Technologists*, Vol. 68, (1999a) pp. 305-318.

20. Meininger, R. C. "Aggregate Test Related to Performance of Portland Cement Concrete Pavement." *National Cooperative Highway Research Program Project 4-20A Final Report.* Transportation Research Board, National Research Council, Washington, D.C (1998).

21. Saeed, A., Hall, J., and Barker, W. "Performance-Related Tests of Aggregates for Use in Unbound Pavement Layers." *National Cooperative Highway Research Program Report 453*, Transportation Research Board, National Research Council, Washington, D.C (2001).

22. Fowler, D. W., Zollinger, D. G., Carrasquillo, R. L., and Constantino, C. A., *Aggregate Tests Related to Performance of Portland Cement Concrete*, Phase 1 Unpublished Interim Report, National Cooperative Highway Research Program (NCHRP) Project 4-20, Lincoln, NE (1996).

23. Lee, J. C., White, D. T., and West, R. T. "Effect of Fine Aggregate Angularity on Asphalt Mixture Performance." *Federal Highway Administration, Indiana Dept. of Transportation, Joint* Transportation Research program FHWA/INDOT/JTRP-98/20, Final Report, West Lafayette, IN (1999b).

24. Indiana University - Purdue University Fort Wayne IPFW Geosciences Website, (www.geosci.ipfw.edu).

25. Jahn, D. "Evaluation of Aggregate Particle Shapes Through Multiple Ratio Analysis." *Proceedings of the 8th Annual Symposium of the International Center for Aggregate Research (ICAR)*, Denver, CO (2000).

26. Kuo, C. Y., Frost, J. D., Lai, J. S., and Wang, L. B. "Three-Dimensional Image Analysis of Aggregate Particle from Orthogonal Projections." *Transportation Research Record 1526*, Transportation Research Board, National Research Council, Washington, D.C. (1996) pp. 98-103.

27. Masad, E., Olcott, D., White, T., and Tashman, L. "Correlation of Fine Aggregate Imaging Shape Indices with Asphalt Mixture Performance." *Transportation Research Record 1757*. Transportation Research Board, National Research Council, Washington, D.C. (2001) pp. 148–156.

28. Brzezicki, J. M., and Kasperkiewicz, J. "Automatic Image Analysis in Evaluation of Aggregate Shape." *ASCE Journal of Computing in Civil Engineering (Special Issue on Image Processing),* (1999). Vol. 13, No. 2 (1999) pp.123–130.

29. Barksdale, R. D., Kemp, M. A., Sheffield, W. J., and Hubbard. J. L. "Measurement Of Aggregate Shape, Surface, Roughness." *Transportation Research Record 1301*, Transportation Research Board, National Research Council, Washington, D.C., (1991) pp. 107-116.

30. Masad, E., Muhunthan, B., Shashidhar, N., and Harman T. "Internal Structure Characterization of Asphalt Concrete Using Image Analysis." *ASCE Journal of Computing in Civil Engineering (Special Issue on Image Processing)*, Vol. 13, No. 2 (1999a) pp. 88 – 95.

31. Masad, E. A., Muhunthan, B., Shashidhar, N., and Harman, T. "Effect of Compaction Procedure on the Aggregate Structure in Asphalt Concrete." *Transportation Research Record 1681*, Transportation Research Board, National Research Council, Washington, D.C., (1999b) pp. 179-184.
32. Li, L., Chan, P., Zollinger, D. G., and Lytton, R. L. "Quantitative Analysis of Aggregate Shape Based on Fractals." *ACI Materials Journal*, Vol. 90, No. 4 (1993) pp. 357-365.
33. Wilson, J. D., and Klotz, L. D. "Quantitative Analysis of Aggregates Based on Hough Transform." *Transportation Research Record 1530*, Transportation Research Board, National Research Council, Washington D.C. (1996)1pp. 11-115.
34. Yeggoni, M., Button, J. W., and Zollinger, D. G. "Influence of Coarse Aggregate Shape And Surface Texture on Rutting of Hot-Mix Concrete." *Texas Transportation Institute Report 1244-6*, Texas A&M University, College Station, TX (1994).
35. Masad, E., Button, J., and Papagiannakis, T. "Fine Aggregate Angularity: Automated Image Analysis Approach." *Transportation Research Record 1721,* Transportation Research Board, National Research Council, Washington D.C. (2000) pp. 66–72.

36. Kuo, C., and Freeman, R. B. "Imaging Indices for Quantification of Shape, Angularity, and Surface Texture of Aggregates." *Transportation Research Record 1721*, Transportation Research Board, National Research Council, Washington D.C. (2000) pp. 57–65.

37. Rao, C., Tutumluer E., and Stefanski, J. A. "Coarse Aggregate Shape and Size Properties Using a New Image Analyzer." *ASTM Journal of Testing and Evaluation*, JTEVA, Vol. 29, No. 5 (2001) pp. 79-89.

38. Hryciw, R. D., and Raschke, S. A. "Development of a Computer Vision Technique for In-Situ Soil Characterization." *Transportation Research Record 1526*, Transportation Research Board, National Research council, Washington, D.C., (1996) pp. 86-97.

39. Wang, L. B., and Lai, J. S. "Quantify Specific Surface Area of Aggregates Using an Imaging Technique." *Transportation Research Board 77th Annual Meeting*, Washington, D.C (1998).

40. Masad, E., and Button, J. "Unified Imaging Approach for Measuring Aggregate Angularity and Texture." *Journal of Computer-Aided Civil and Infrastructure Engineering*, Vol. 15, No. 4 (2000) pp. 273-280.

41. Yeggoni, M., Button, J.W., and Zollinger, D.G. "Fractals of Aggregates Correlated with Creep in Asphalt Concrete." *Journal of Transportation Engineering (ASCE)*, Vol. 122, No. 1 (1996) pp. 22-28.

42. Rao, C., and Tutumluer, E. "A New Image Analysis Approach for Determination of Volume of Aggregates." *Transportation Research Record 1721*, Transportation Research Board, National Research Council, Washington, D.C., (2000) pp. 73-80.

43. Browne, C., Rauch F. A., Haas T. C., and Kim H. "Comparison Tests of Automated Equipment for Analyzing Aggregate Gradation." *Proceedings of the 9th Annual Symposium of the International Center for Aggregates Research (ICAR)*, Austin, TX (2001).

44. Maerz, N., Palangio, H., and Franklin, J.A. "Wipfrag Image Based Granulometry System." *Proceedings of the FRAGBLAST 5*, Workshop on Measurement of Blast Fragmentation, Montreal, Quebec, Canada, (1996) pp. 91-99.

45. Maerz, N. H., and Lusher, M. "Measurement of Flat and Elongation of Coarse Aggregate Using Digital Image Processing." *Transportation Research Board Proceedings*, *80th Annual Meeting*, Washington D.C., Paper No. 01-0177 (2001).

46. Rao, C., Tutumluer, E., and Kim, I. T. "Quantification of Coarse Aggregate Angularity Based on Image Analysis." *Transportation Research Record 1787*, Transportation Research Board, National Research Council, Washington, D.C., (2002) pp. 117-124.

47. Fletcher, T., Chandan, C., Masad, E., and Sivakumar, K. "Measurement of Aggregate Texture and Its Influence on HMA Permanent Deformation." *Journal of Testing and Evaluation, American Society for Testing and Materials, ASTM*, Vol. 30, No. 6, (2002) pp. 524-531.

48. Kim, H., Haas, C. T., Rauch, A. F., and Browne, C. "Wavelet-Based 3D Descriptors of Aggregate Particles." *Transportation Research Record 1787*, Transportation Research Board, National Research Council, Washington, D.C. (2002) pp. 109-116.

APPENDIX E

PHOTOGRAPHS OF AGGREGATE SAMPLES

Aggregate 1 (#8 [2.36 mm] - #16 [1.18 mm])

Aggregate 2 (#8 [2.36 mm] - #16 [1.18 mm])

Aggregate 5 (#8 [2.36 mm] - #16 [1.18 mm])

Aggregate 6 (#8 [2.36 mm] - #16 [1.18 mm])

Aggregate 10 (#8 [2.36 mm] - #16 [1.18 mm])

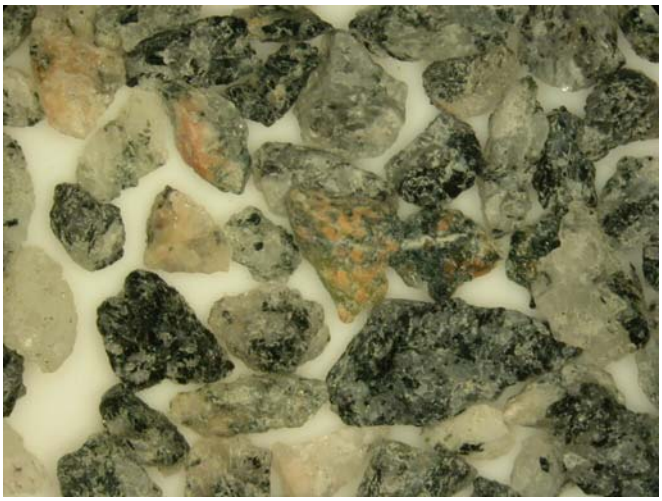

Aggregate 1 (3/4” [19.0 mm] - 1/2” [12.5 mm])

Aggregate 2 (3/4” [19.0 mm] - 1/2” [12.5 mm])

Aggregate 3 (3/4” [19.0 mm] - 1/2” [12.5 mm])

Aggregate 4 (3/4” [19.0 mm] - 1/2” [12.5 mm])

Aggregate 5 (3/4” [19.0 mm] - 1/2” [12.5 mm])

Aggregate 6 (3/4” [19.0 mm] - 1/2” [12.5 mm])

Aggregate 7 (3/4” [19.0 mm] - 1/2” [12.5 mm])

Aggregate 8 (3/4” [19.0 mm] - 1/2” [12.5 mm])

Aggregate 9 (3/4” [19.0 mm] - 1/2” [12.5 mm])

Aggregate 10 (3/4” [19.0 mm] - 1/2” [12.5 mm])

Aggregate 11 (3/4” [19.0 mm] - 1/2” [12.5 mm])

Aggregate 12 (3/4” [19.0 mm] - 1/2” [12.5 mm])

Aggregate 13 (3/4” [19.0 mm] - 1/2” [12.5 mm])